Phase I Final Report

Development of Test Procedures to Determine Emissions from Open Burning of Agricultural and Forestry Wastes

Prepared for the
California Air Resources Board

Contract No. A5-126-32
January, 1990

Principal Investigators

Bryan M. Jenkins
Daniel P.Y. Chang
Otto G. Raabe

Co-Investigators

A. Daniel Jones
George E. Miller

Research Staff

Scott Q. Turn
Robert Williams
Steve Teague
James Mehlschau
Nancy Raubach
Dale Uyeminami

University of California
Davis, California 95616

Abstract

Recent legislation in California requires the development of procedures to determine the magnitudes of emission offsets available to power plants and other facilities which burn biomass fuels, including agricultural crop wastes and wastes from forestry operations normally open burned in the field for disposal. Previously determined emission factors require verification or updating, and additional types of fuels need to be tested. To simulate the conditions under which open fires are conducted in the field, a large wind tunnel incorporating a combustion test section was developed. The wind tunnel provides a means of controlling the variables which most influence fire behavior in the field, these being fuel type, fuel moisture, fuel bed structure, fuel loading rate, and wind speed. The simulator permits the combustion products to be channeled through a sampling duct for evaluating emissions of particulate matter, CO, hydrocarbons, NO_x, SO_2 and other volatile species. All residual ash from the fire can be collected for analysis. The design utilizes a moving fuel bed to generate a flame which is stationary in space. In principle, this allows a test of any duration to be conducted. Emission factors can therefore be based on the combustion of much larger quantities of fuel than previously possible except under the variable conditions of actual field burns. The tunnel also includes a wettable floor to simulate soil conditions beneath the fire.

To evaluate the simulator, two experiments were performed on rice straw. These tests were conducted under similar conditions of fuel moisture, fuel loading rate, and wind speed. Both fires were conducted as backing fires, with the fire propagating in opposition to the wind, in the manner required

for open burning of straw materials. The repeatability of the fire propagation velocity and emission data was good. Results were also comparable to data from field and laboratory experiments, except for discrepancies in particulate, NO_x, and SO_2 concentrations reported from previous simulator trials.

Further testing is required to determine the optimal operating configurations of the tunnel for the purposes of generating representative emission factors. The conditions imposed on the fire can be varied, and the preliminary tests conducted to date are insufficient to demonstrate the influences of these conditions on the fire behavior or the emissions from the fire. Additional research is needed to understand these influences so as to select appropriate operating conditions for future experiments.

Table of Contents

Title Page	1
Abstract	2
Table of Contents	4
List of Figures	5
List of Tables	7
Acknowledgements	8
Summary and Conclusions	9
Recommendations	13
Introduction	15
Background	20
Wind Tunnel Development	28
Prototype Development	31
Large Scale Tunnel Development	33
Flow and Fire Characterization	38
Emissions Testing	51
Results	58
Discussion	64
References	68
Nomenclature	72
Tables	
Figures	

List of Figures

1. Schematic of the UCD prototype wind tunnel for maintaining stationary open flames.

2. Frequency of the wind for Woodland, CA during September and October, 1987.

3. Exterior design view of the large scale wind tunnel.

4. Photograph of the large scale wind tunnel showing flow development section, combustion test section, sampling stack, and instrument trailer.

5. Wall thermal dissipation rate (dimensionless) as a function of the wind tunnel width.

6. Schematic of the fuel conveyor system for the large scale wind tunnel.

7. Vertical velocity profile and turbulence intensity at the entrance to the combustion test section. Shown for comparison is the computed turbulence intensity of the field estimated for a grass surface.

8. Horizontal velocity profile and turbulence intensity at the entrance to the combustion test section.

9. Lateral velocity profile and turbulence intensity across the sampling stack.

10. Longitudinal velocity profile and turbulence intensity across the sampling stack.

11. Comparison of the actual inlet vertical velocity profile to a logarithmic law of the wall profile based on a 5 cm high grass surface ($u* = 0.32$, $z_o = 0.02$, $d_o = 0$).

12. Temperature at the fuel surface for field burns in rice straw conducted as backing (a) and heading (b) fires. Data from two thermocouples separated horizontally by 0.95 m are shown.

13. Temperature contour maps generated from a vertical array of thermocouples during field tests of backing (a) and heading (b) fires in rice straw. The vertical (elevation) scale is exaggerated.

14. Wind tunnel temperature histories for fires in rice straw burning past a thermocouple at the fuel surface: (a) fuel carried on the rod conveyor and open below, with the ceiling extended to the leading edge of the fire, (b) ceiling extended but with a steel sheet inserted just below the rod conveyor, (c) ceiling retracted with the fuel bed open from below, and (d) ceiling retracted with a steel sheet inserted below the rod conveyor.

15. Sampling train used to collect particulate, volatile organic, and gas samples from the sampling stack of the large scale wind tunnel.

16. Inlet air conditions for the tests of 1 and 7 September, 1988.

17. Stack temperatures at the sampling port during the tests of 1 and 7 September, 1988.

18. Temperatures measured at 216 mm above the leading edge of the fire during the tests of 1 and 7 September, 1988.

19. Temperatures measured at 44 mm above the leading edge of the fire during the tests of 1 and 7 September, 1988.

20. Sample chromatogram (sorbent tube #1) taken during the test of 7 September and analyzed by GC-MS.

21. Scanning electron micrograph of sample drawn from the pyrolysis zone of the fire. Sample was collected with a point to plane electrostatic precipitator on a carbon coated electron microscope grid. Residues of droplets containing solid material are visible.

22. Scanning electron micrograph of sample drawn from the pyrolysis zone of the fire. Sample was collected with a point to plane electrostatic precipitator on a carbon coated electron microscope grid. Residues of fine droplets are visible.

23. Transmission electron micrograph of particulate material collected from the pyrolysis zone of the fire. Fine chain aggregate along with droplet residues are visible.

24. Transmission electron micrograph of particulate material collected from the pyrolysis zone of the fire. Residues from fine droplets containing solid material are visible.

25. Scanning electron micrograph of samples from behind the flame collected on a Nuclepore filter and showing fine chain aggregate.

26. Scanning electron micrograph of samples from behind the flame collected on a Nuclepore filter. Visible is a large flyash particle with other combustion particles aggregated on its surface.

27. Scanning electron micrograph of sample drawn from the incandescent region of the fire behind the flame in the fuel bed. Sample was collected with a point to plane electrostatic precipitator on a carbon coated electron microscope grid.

28. Transmission electron micrograph of sample drawn from the incandescent region of the fire behind the flame in the fuel bed. Sample was collected with a point to plane electrostatic precipitator on a carbon coated electron microscope grid.

List of Tables

1. Fuel and ash analysis for combustion trials of 1 September and 7 September, 1988, in rice straw.

2. Material balances and fire characteristics for tests of 1 September and 7 September in rice straw.

3. Particulate concentrations and size distributions for combustion trials of 1 September and 7 September, 1988, in rice straw.

4. Emission factors (kg/t) for combustion trials of 1 September and 7 September, 1988, in rice straw, with comparison to Darley [1979].

Acknowledgements

The authors acknowledge the support and cooperation of the California Air Resources Board in conducting this project. The efforts of Jack Paskind and Manjit Ahuja are especially appreciated.

James Mehlschau, Senior Development Engineer of the Agricultural Engineering Department, UC Davis, was responsible for translating the design concept for the large scale wind tunnel into a working device. He was also responsible for the acquisition of all materials and the final erection of the tunnel. The rapidity with which various design changes were implemented after assembly were due primarily to his efforts. Fabrication of the tunnel was done by Lowell Jahn, Charles Barden, Brett Anglin, Burt Vannucci, and Richard Miller of the Agricultural Engineering Department. Their considerable expertise was much in evidence during the fabrication and erection of the tunnel. Assistance in fabrication was provided by Jim Mehlschau and Scott Turn. On site management of the experimental phase was done by Turn with assistance from Rob Williams and Eduardo Pellegrina. Stack sampling was performed by Steve Teague, who also analyzed the particulate filters and computed the log-normal distributions. Teague also conducted the electron microscope studies of the particles collected from the prototype tunnel. Dale Uyeminami analyzed the sorbent tubes on the GC-MS. Nancy Raubach performed the GC analyses on the stack gas grab samples collected. Dan Jones of the Facility for Advanced Instrumentation contributed substantial time and advice during the conduct of the analyses using the electron microscopes and the GC-MS.

Summary and Conclusions

A large-scale wind-tunnel combustion-simulator was constructed for the purpose of generating emission factors for pollutants emitted during the open burning of agricultural and forestry wastes. These emission factors are to be used in determining the magnitude of emission offsets granted to facilities using biomass fuels that would otherwise be openly burned for disposal.

The wind tunnel was developed to test both spreading-type fires (those propagating through a fuel bed such as a cereal grain crop residue) and pile-type fires (typical of the burning of tree prunings) . For spreading-type fires, the tunnel design incorporated a traveling fuel bed developed with the intent of generating a uniformly propagating flame front similar to those observed in proper field burns in backing or strip-lighted mode. Also included was a wettable refractory floor to simulate dry or wet soil conditions under the fire. The tunnel is of an open circuit, forced draft type employing a 45 kW centrifugal blower to generate a maximum mean wind speed of 5 m/s through a duct 1.2 meters square in cross section. In operation, the fuel is loaded ahead of the blower and onto a primary fuel conveyor which moves along the floor of the 10 m long flow development section. At the end of the flow development section, the fuel is transferred to a stainless steel rod conveyor and into the combustion test section. This section is 7.3 m long and extends nearly 4 m vertically before narrowing into the sampling duct 8 m above the fuel surface. Beneath the rod conveyor is a secondary stainless mesh conveyor to intercept burning fine material descending through the upper conveyor and transport

the material downstream at the same velocity. This conveyor was necessary to avoid early ignition of incoming fuel. In addition to this open conveyor configuration, a floor can be imposed directly below the fuel to prevent ventilation from underneath. All conveyors are driven at the same linear velocity by a variable speed DC motor adjusted to match the natural propagation velocity of the fire. In this manner, the flame can be made to remain stationary in space for extended sampling periods. The wall of the combustion test section is lined with doors which may be opened to permit inflow of air from all directions during pile burns under no wind conditions. Each door contains two windows to allow viewing the fire when the doors are closed. The windows also act as noncatalytic walls during the conduct of spreading fires using the fuel conveyors to generate a stationary flame.

Two acceptance tests were performed in addition to a number of preliminary tests of the tunnel apparatus. The acceptance tests were done to evaluate the repeatability of data obtained under similar wind and fuel conditions. Particulate concentrations and size distributions were determined using two cascade impactors in parallel. Concentrations of oxides of nitrogen, sulfur dioxide, and carbon monoxide were determined using on-line electronic gas analyzers. Grab samples for low molecular weight hydrocarbon and carbon dioxide analyses were taken and analyzed by gas chromatography (GC). Benzene was analyzed by passing a stream of gas from the sampling duct through sorbent tubes packed with Tenax/Ambersorb, and comparing the results from gas-chromatography/mass spectrometry (GC/MS) against similar tubes loaded with standards. Qualitative identification was also obtained for several other volatile organic compounds. The tests were performed by burning rice straw at approximately 7% moisture (wet basis) at a loading rate

of 600 g/m^2 in a wind of 2.35 m/s mean velocity. The boundary layer development up to 35 cm above the fuel bed in the flow development section was seen to match a logarithmic law of the wall profile using friction velocity and surface roughness coefficients reported in the literature for a 5 cm tall grass surface. Flow in the sampling stack was observed to be of uniform velocity and turbulence intensity across the duct section. Emission factors obtained for both tests were comparable. Particulate emissions were on the order of 3 kilograms per metric ton (kg/t), NO_x was 2.2 kg/t (as NO_2), SO_2 was 0.16 kg/t, hydrocarbons including benzene were 2.2 kg/t, and CO was emitted at 60 kg/t. Benzene concentrations were on the order of 100 ppb in the stack. After methane, ethene at 0.6 kg/t was the next highest concentration of hydrocarbon emission. In comparison to data reported by an earlier study (Darley, 1979), particulate emissions were higher, benzene emissions were higher, while NO_x and SO_2 emissions were lower, although there exist discrepancies in the data reported for rice straw by Darley [1979] and Darley [1977]. Darley [1977] reports 3.47 kg/t particulates for rice straw burned in backing mode, instead of the 1.06 kg/t reported in Darley [1979]. Values for SO_2 reported by Darley [1979] were also computed by mass balance on sulfur, and do not represent actual measurements of SO_2 concentrations in the combustion products. Particulate size distributions show that 90% of the particles are less than 4 μm in diameter, and 80% are less than 1 μm. These results are in excellent agreement with distributions observed from field collected samples (Goss and Miller, 1973). In addition, the time-temperature relationships for the fires in the wind tunnel and the field are similar.

Further testing is required to isolate any effects of quenching which may exist as a result of the fuel conveyors or the tunnel walls and which

might lead to higher concentrations of volatile organics. In general it appears that the wind tunnel combustion simulator can be used to generate emission factors under more carefully controlled conditions of wind and fuel than previously possible, and that many of the individual effects of fuel and environment on the fire behavior can now be better understood. Further work is required to determine the best operating configurations for the wind tunnel to match field conditions.

Recommendations

Preliminary tests in the wind tunnel and a review of the tunnel design indicate that the facility can be used to reproduce emissions from open burning (Williams, 1989). The tunnel can be operated in a number of different configurations in an effort to best match wind and fuel conditions in the field. Further testing should be carried out to understand how the different operating configurations influence the emission characteristics. Specific experiments should be conducted to evaluate the effect of ceiling position and type of floor on fire propagation and emission factors. The inlet air velocity profile above 35 cm indicates that additional roughness may need to be added in the tunnel flow development section to increase boundary layer depth and possibly turbulence intensity, although current values are within the range reported in the literature. Experiments are needed to test the effect of increased roughness on emission production.

Additional testing should be performed to identify what effects the walls and conveyor elements have on quenching and the emission of volatile organics from the fire. This can be done by sampling from the flame region alone to avoid the effects of the walls, and by burning without the conveyor to avoid the effects of quenching on the conveyor rods.

The SO_2 concentrations are also well below what was expected on the basis of previously published emission factors. The use of source sampling equipment as anticipated has not proved necessary, and an ambient level analyzer should be employed.

The two cascade impactors used gave somewhat different particle size distributions, although the total particulate concentrations were similar. Data from the high temperature, high pressure cascade impactor appears more repeatable. Further testing is required to evaluate the performance of the second impactor.

With an understanding of the above effects, evaluation of other fuel materials can proceed. Further experiments can be conducted to determine emission factors for the major crop and forest residues proposed as fuel for biomass facilities. As well as sampling for emissions described in this report, additional materials should be examined, including other PAH materials and possibly polychlorinated dioxins and furans. Particulate matter should be further characterized in terms of organic and inorganic species which may be present on or in the particles. Relevant effects of fuel moisture, fuel bed structure, fuel loading rate, wind velocity, air temperature and humidity, and moisture status of the underlying floor should also be explored to understand the fire dynamics and the influence of heterogeneous field conditions on the emission factors.

Introduction

State legislation enacted in 1983 under Assembly Bill 1223 directed the California Air Resources Board to develop procedures to determine the magnitudes of emission offsets available to facilities which burn biomass for the generation of steam or electricity. AB 1223 added Section 41605.5 to the California Health and Safety Code requiring districts to include incremental emission benefits in considering any offset requirements for projects in which biomass is used as fuel.

This legislation was introduced in recognition of the potential reduction in air emissions from open field burning of crop and forest waste biomass resulting from typical agricultural and silvicultural practices in the state. Increased activity in the development of biomass fueled facilities occurred after the enactment of the federal Public Utilities Regulatory and Policy Act of 1978 which increased incentives provided by utility companies for the purchase of energy and capacity from third party developers.

In satisfaction of AB 1223, the ARB in 1984 created a guideline procedure for calculating the magnitude of available offsets. This procedure was later modified in 1988 in response to AB 2158 [CARB, 1988]. The ARB procedure for calculating the offsets is of the form:

$$P = \frac{x}{365} \sum_{i=1}^{12} \sum_{j=1}^{n} B_{ij}\, EF_j\, HBF_j \qquad \{1\}$$

where x is a fraction corresponding to the allowable offset as determined by the proximity of the biomass to the facility, B_{ij} is the quantity (tonnes) of biomass of type j used during month i, EF_j is the emission factor of pollutant in kg/t of biomass j which is open burned, HBF_j is the fraction of total biomass j that is open burned, and P is the pollutant offset credit in kilograms per day. A value P is computed for each type of pollutant which may be offset. The parameter x takes on the value 1/2 for biomass originating more than 24 km away from the plant, and 1/1.2 for biomass from within 24 km of the facility.

The present study is concerned with methods to determine the emission factors, EF_j, of equations {1}. Other work is concerned with the development of factors HBF_j pertaining to the fraction of biomass actually field burned, and this matter is not further discussed here. Nor is the question of emission profiling (the distribution of emissions from open burning throughout the year) addressed here, although it may be recognized that the time of burning can indirectly influence the emissions from burning due to environmental influences on such attributes as fuel moisture, fuel bed structure, air relative humidity, air temperature, wind speed and direction, and soil moisture status. The work undertaken in this project was designed to elucidate the effects of the fuel and environmental conditions on the emission factors required for equations {1}. To this end, a procedure for conducting the burning and the emission sampling was required to reduce uncertainty associated with uncontrolled internal and external parameters of the fire.

The approach adopted was to empirically simulate the open burning process, but in a manner compatible with the goals of controlling the major variables affecting the fire. Open burning of agricultural and forestry wastes

is principally done in one of two forms: spreading fires and pile burns. For field crop residues which are generally spread behind the crop harvesting equipment in a layer distributed over the soil and stubble surface, the burning is done as a fire front which is allowed to propagate naturally into the fuel bed. Current regulations in California call for this burning to be done in either backing or strip lighted mode. For backing fires, the direction of fire propagation is directly opposite the direction of the wind, and this is largely true for strip lighted fires as well. The benefits of these techniques in reducing particulate emissions have been shown to be substantial when compared to the emissions from so called heading fires, in which the direction of fire propagation is concurrent with the direction of the wind. In backing fires, the fire propagation velocity is thought to be less sensitive to the wind velocity, whereas, in heading fires, the fire velocity is directly proportional to the wind velocity due to heat transfer from the flame overlying the unreacted fuel bed. Volatiles emitted from the fuel during heating and pyrolysis prior to ignition are also more likely to escape the flame in a heading fire. For these reasons, burning against the wind is the adopted practice for field crop residues.

For orchard prunings and much of the forest slash, pile burns are conducted. These fires are set after the biomass has been pushed into a pile, generally at the edge of the field. Ignition may be initiated at several locations around the pile such that the fire propagates into the pile from the periphery, and involves much of the fuel simultaneously throughout the duration of the burn. The pile represents a point source of emissions, as compared to the line or area sources occurring with spreading fires of field crop residues.

In both situations, the fire will induce it own draft. It will also respond to an impressed wind which is almost always present to some extent. Also, emissions continue after the passage of the initial flame front, generally as a smoldering afterburn. In spreading fires of field crop residues, these secondary emissions may continue for some time as a result of non-uniform deposition of residue. Where deep piles of residue have accumulated or been deposited, the short residence time of the fire and the reduced diffusion of atmospheric oxygen into the pile contribute to the prolonged emission. The structure of the fuel bed therefore has an influence on both the primary and secondary emissions from the fire. In addition to the direction and magnitude of the wind, and the fuel bed structure, other major parameters which influence the emissions from the fire include fuel type, fuel moisture, fuel morphology, and the condition of the soil surface beneath the fire. This surface can serve as a source of extinction and as a source of moisture. The influence is probably greater on spreading fires than on large pile burns, but may have some effect none the less.

To simulate the major influences on the fire, a wind tunnel was constructed which was capable of supporting both spreading and pile type fires. This tunnel was in some respects similar to other wind tunnels used elsewhere to study the fire propagation velocity in spreading type fires. Most of these tunnels had stationary floors and rather limited duration testing capabilities, which was seen to be undesirable from the standpoint of emissions monitoring because of the very small sample sizes involved. The UCD tunnel includes a moving floor which can be used when conducting spreading fires. By moving the floor, the fire can be made to propagate

indefinitely into the fuel bed introduced into the upstream end of the tunnel. Emissions sampling can then occur for as long as necessary to capture representative samples or to integrate the emission load over the anticipated duration of an actual field fire. Primary emission sampling is done in a stack some 8 m (26 feet) above the fire. When testing spreading fires with an impressed wind, the gas temperature in the stack runs about 15 K above the temperature of ambient air entering the tunnel. The data collected therefore are representative of emission levels in the plume shortly after quenching, and do not include any longer term effects due to atmospheric reactions occurring far behind the fire. These may be understood to some degree from the primary emissions. The tunnel provides a means to control the factors influencing the fire and thus permits the study of how changes in the condition of the fire affect the emission levels observed, a study which is virtually impossible to conduct in the field.

This report describes the design of the wind tunnel and initial experiments conducted to determine if repeatable emission rates could be obtained under separate tests. Tunnel fabrication and preliminary testing were completed as an initial phase of a program to develop emission factors for various biomass fuels commonly burned in the field in California. The objective was to determine if a repeatable method could be developed to determine these emission factors. Subsequent phases of the program are intended to carry out the actual determination of the emission factors and to understand how changes in the condition of the fuel, the wind, and the soil influence the emission rates of pollutants from the fire.

Background

Currently, the two main sources of information on emission factors from agricultural and forestry wastes which are allowed for the purposes of equation {1} are the U.S. Environmental Protection Agency's Compilation of Air Pollutant Emission Factors [EPA, 1973], and the report Hydrocarbon Characterization of Agricultural Waste Burning by E.F. Darley [1979]. To update the emission factor database and to reduce the uncertainty associated with the assignment of offset credits, the California Air Resources Board contracted with the University of California, Davis in June, 1986 to develop an improved test procedure for determining emission factors from agricultural and forestry wastes. Specific information was requested on emissions of particulate matter (PM 10), carbon monoxide, oxides of nitrogen, sulfur dioxide, and hydrocarbons. Concentrations of benzene were of particular interest.

Darley's data were developed from fires conducted in an instrumented natural draft burning tower. Both pile type and spreading fires were conducted on a stationary platform situated beneath a large hood used to conduct the combustion products through a sampling stack [Darley, et al., 1966; Darley, 1972; Darley, 1977; Darley, 1979]. Darley carried out tests on 31 types of field crop residues, vine and orchard prunings, and weeds. For field crop residues, fires were conducted using about 2.7 to 3.6 kg of fuel. Heading fires and backing fires were simulated by burning on a sloped surface: heading fires burned up slope and backing fires burned down slope. Higher wind speeds were generated by ventilating across the fuel surface with the draft of a standard household fan. Orchard prunings were burned in piles with both a

"cold" ignition and a "roll on" ignition. The latter was conducted by "rolling" the new pile of prunings onto the hot coals of the previous fire. This was intended to simulate the field practice of adding new material to an existing fire.

In earlier work [Darley, 1977], Darley generated data on emissions of particulate matter, CO, and total hydrocarbons. Results of these studies substantiated benefits of backing fires relative to heading fires in field crop residues in reducing total emission of particulates, although the mass mean diameter of the particulate was reduced by a factor of 2 (from 0.22μm to 0.11μm). The role of fuel moisture was also explored, showing no apparent advantage in drying orchard prunings below about 35% moisture, but showing a large advantage in burning field crop residues at as low a moisture content as possible.

In a later study [Darley, 1979], Darley analyzed hydrocarbon emissions from five field crop residues and three orchard crop residues. He also analyzed for particulate matter, NO, NO_2, CO, and attempted to analyze SO_2, although direct analysis was unsuccessful. The SO_2 values given were computed by assuming that the sulfur deficit from an elemental balance between the fuel and the residual char could be attributed to the emission of SO_2 from the fire. Darley indicated that this assumption was known to be invalid because chromatographic analysis had indicated the presence of small but variable concentrations of H_2S and another, unidentified, sulfur compound. Neglecting emission of oxides of sulfur in a manner consistent with EPA was considered by Darley to be appropriate for some materials, but

for others the sulfur deficit was high enough to indicate the need for more advanced analysis.

Speciation of hydrocarbons indicated that saturated hydrocarbons were the most prevalent up to C_6. Olefin yields were approximately half that of the saturated hydrocarbons, and ethene accounted for 70% of the olefins. Of the hydrocarbons C_6 and above, benzene was the compound found in highest concentration, and the only one exceeding 0.25 kg/t.

The burning tower of Darley was also used in other investigations of emissions from open burning of various biomass materials. This facility was used by Boubel et al. [1969] in a study of the emissions from open burning of grass stubble and straw. Burning tower results were also reported by Carroll et al. [1977] and by Goss and Miller [1973]. Mast [1986] used the same tower in a study of the mutagenicity and chemical characterization of organic materials on particulate matter generated by burning rice straw. Mast also compared her results from the burning tower simulations to samples collected from plumes of actual fires. The indirect mutagenic activity of the samples collected from the burning tower was approximately four times that of the activity of samples collected from the field burns. The extractable organic matter was also lower for the burning tower experiments. Mast hypothesized that the discrepancy was due to the difference in the quench rate of the combustion gases above the fire. In the field, the combustion gases are cooled quickly, with temperatures approaching ambient about 1 m above the flame, and certainly within the first 10 m above the flame [Carroll, et al., 1977]. In the burning tower experiments, the gas temperature at the neck of the hood and approximately 3.5 m above the fire was as high as 280°C, and as high as 150°C

at the sampler intakes. These conditions were thought to favor secondary reactions or more complete combustion with distribution of organic compounds to the vapor phase (hence the lower extractable content of the particulate matter). The burning tower experiments had been conducted by burning down the inclined fuel surface to simulate backing fires. The field burns were also conducted in backing fire mode.

Several attempts have been made to characterize the emission rates using data collected from fires in the field, rather than from the laboratory. Boubel, et al., [1969] sampled 12 field burns in five different types of grasses for comparison with data obtained from experiments in Darley's burning tower. Yields of particulate matter from the burning tower ranged from 4.5 to 13 kg/t of fuel burned. Particulate yields from field burns were 0.7 to 7.8 kg/t with the exception of one fire which yielded 40.6 kg/t. A study by Goss and Miller [1973] also demonstrated a tendency towards reduced particulate matter yields from field burns of rice straw compared to burning tower trials. Studies conducted under the auspices of the Oregon Department of Environmental Quality [1979] showed higher particulate emission rates, however, with values of 10.5 to 81.5 kg/t for backing fires in perennial ryegrass residue between 5 and 16% moisture content wet basis. In both the Oregon study and that conducted by Goss and Miller, the emission factors were computed on the basis of carbon balances on the fuel and the product gases, and are therefore sensitive to the determination of or assumptions about the CO_2 concentrations in the gas phase effluent of the fire. Inaccurate determination of CO_2 concentration, which is near ambient in the plume, causes closure problems on the mass balance, and hence may cause underestimation or overestimation of total fuel mass burned.

Carroll [1973] and Carroll, et al. [1977] conducted aircraft penetration studies in plumes from field burns. These were used to characterize the three dimensional atmospheric thermal structure and measure the water vapor and particulate matter distribution. Penetration of fire plumes from backing fires showed the unexpected result of temperature rises in the plume relative to its horizontal environment of only 0.1 K or less at elevations of 30 to 100 m. For heading fires, plumes were somewhat warmer at these elevations, with temperature excesses of from 0.5 to 3.0 K. The temperature excess decreased with increasing wind speed, and were reported by Carroll to be comparable to those associated with normal thermal activity in the area. Carroll also found that measurement of the wind at an elevation of 2 m above the ground appeared to be sufficient to define plume behavior. Carroll also noted that heading fires could be characterized by emissions from both the flaming stage and the smoldering afterburn stage, whereas emissions from the afterburn stage in backing fires were considerably reduced or absent.

The rapid decrease in temperature within the plume above field fires led Carroll, et al. [1977] to conclude that condensation processes contribute significantly to the plume particulate concentrations. With rapid cooling due to ambient air entrainment and radiation losses, many of the higher molecular weight species condense, adding a large number of liquid and solid condensates to the particulate load. As the plume continues to rise, ambient air entrainment lowers the average gas phase mixing ratio, thereby reducing the vapor pressure over the condensed phase material. As a result, re-evaporation of liquid droplets would occur. Particulate matter sampled shortly

above the flame therefore may be only partially indicative of particle concentrations and character farther downstream from the fire.

Wind tunnel studies of open burning have been conducted in an effort to understand the character of natural forest fires and to improve predictions of fire propagation in combating such fires. Experimental studies have led to development of mathematical models of fire spread in a number of different types of fuels. Most of these models are empirical in nature, although attempts have been made to derive the fire propagation velocity from first principles. Rothermel conducted extensive tests in a laboratory study on fire propagation behavior [Anderson and Rothermel, 1965; Rothermel and Anderson, 1966; Mobley, 1976] and developed empirical models of the behavior to be used in predicting the spread of the fire as a function of wind speed, fuel moisture, and fuel type [Rothermel, 1972; Rothermel, 1983]. Rothermel's experiments were conducted in a laboratory facility that included a burning platform similar to Darley's, as well as low speed and high speed wind tunnels used to simulate wind conditions experienced in the field [Rothermel, 1967]. These tunnels were constructed so that a stationary fuel bed could be burned with a fire moving relative to the floor of the laboratory. The objective was to determine the burning rate and the propagation velocity, and no information was presented regarding emissions from the fires, although emission data for forest fires is reported in Mobley [1976]. Total suspended particulate matter emission factors tend to be similar to those reported elsewhere for field burns (10 to 90 kg/t depending on fuel moisture, loading rate, and wind characteristics). Emissions of SO_2 were reported to be negligible with the possible exception of fires occurring in high sulfur peat or muck soils. Emissions of benzo(a)pyrene were reported to be considerably higher with

backing fires in slash pine than with heading fires, particularly with light fuel loadings. The differences were attributed to the higher temperatures, lower oxygen concentrations, and longer residence times for backing fires relative to heading fires. Within heading fires, the smoldering afterburn stage produced greater amounts of benzo(a)pyrene and particulate matter than the flaming stage of the fire.

Comparisons of the behavior of prescribed fires with the behavior predicted by Rothermel's model were described by Sneeuwjagt and Frandsen [1977]. The rate of spread determinations were shown to be in good agreement, although there were differences in the flame length and combustion zone depth. These differences were attributed to less accurate determinations of these parameters in the field compared to the laboratory. Albini [1976] summarized a number of modeling techniques for estimating the behavior of wildfires, most based on the methods of Rothermel [1972].

Perhaps the earliest modelling attempt was that of Fons [1946] based in part on the experiments carried out by Curry and Fons [1938]. Fons undertook this effort to understand the fundamental principles governing the rate of fire spread in forest-type fuels. He observed that under field conditions, none of the important factors, such as attributes of the atmosphere, the arrangement of the fuel bed, and the physical properties of the fuel particles remained sufficiently uniform throughout an experiment to allow exact description of the numerous variables influencing the rate of fire spread. For this reason, experimental validation of the model he developed was conducted in a wind tunnel in fuel beds 1 m wide by 2.4 or 3.7 m long. Fires in pine needle litter were directly simulated using beds 50 mm deep. Fires in standing

brush were conducted with uniform arrays of vertical twigs 190.5 mm in length. In modelling the fire, Fons visualized the fire proceeding as a series of successive ignitions with the magnitude of fire spread controlled primarily by the ignition time and separation distance of fuel particles. Fons achieved reasonable agreement between the calculated rate of spread and the experimental rate of spread obtained under similar conditions in the wind tunnel.

Emmons [1964] also developed a thermal model of the propagation of a fire front through forest fuels. This model and the model of Fons [1946] were later described by Emmons and Shen [1971] as ineffective in describing experimental results obtained from burning studies conducted in beds of paper arrays with a well described geometry. The theory of Hottel, et al. [1965] was used by Emmons and Shen and was considered basically correct in describing the relationships among spread rate, burning zone width, and flame length. An attempt to make a more complete theory failed because of inadequate development of the burning zone properties. A unique feature of the experimental program of Emmons and Shen was the use of a moving fuel array to maintain the position of the flame stationary in space. This is similar to the technique developed independently for the design of the wind tunnel utilized in the current study.

The model of Rothermel [1972] used as a basis the approach of Frandsen [1971], a thermal balance model which included flame radiation effects. A more fundamental approach was utilized by Wichman, et al. [1982] in describing the spread rate and the effect of the gas phase velocity profile over the bed. Other contributions to understanding the behavior of fire

propagation through beds of solid fuels have been made by de Ris [1969], McAlevy and Magee [1969], Kosdon, et al. [1969], Berlad, et al. [1971], Lastrina, et al. [1971], Williams [1982], among others. Apparently, no one has yet formulated a fundamental model of emission rates from fires of similar type.

Wind Tunnel Development

Design of the combustion wind tunnel was based on the need to determine and control variables of the fuel and the fire environment in order to understand the effects of these variables on the emission rates observed. The use of a wind tunnel was intended to enable well prescribed conditions that could not be obtained under similar field experiments where the spatial and temporal variation of the major parameters influencing the fire are large, and the difficulties of sampling a moving emission stream in the case of a spreading fire are severe. Fleeter, et al. [1984] were also aware of the difficulties involved in testing hypotheses related to the spread of free burning fires. The tunnel developed here is in several respects similar to that utilized by Fleeter, et al., and as described in some detail by Carrier, et al. [1984]. Fleeter's interest was in modeling the spread of large urban fires generated after the detonation of nuclear weapons. Data obtained from their experiments were intended to contribute to understanding the so-called "nuclear winter" hypothesis pertaining to the reduction in sunlight received at the ground after a nuclear exchange which would result in large amounts of dust and smoke from fires being injected into the atmosphere. The major focus was therefore on providing unimpeded development for strongly buoyant plumes generated by large fires propagating concurrently with the wind (heading fires). The case of spread against the wind was recognized as being important at low crosswind velocities, but was not included in the

analysis. This differs from the simulation of field burns of crop residues in which fires are propagated against the wind by specific intent to reduce the formation of particulate emissions. Even so, the need to provide for the unimpeded expansion of the plume behind the fire in the wind tunnel remains. Fleeter, et al., also recognized that the use of closed channel wind tunnels could lead to recirculation behind the flame front which would not occur in the field. Open channel tunnels would lead to deceleration of the jet like flow at the exit of the flow development section and to variable wind velocity as the flame moved downstream. To deal with this problem, a semi-open channel was devised consisting of a large volume combustion test section incorporating a movable ceiling which was positioned at the leading edge of the plume. The plume was then free to expand beyond the ceiling, and the problems of recirculation and turbulent mixing effects generated by closed and open channel tunnels were avoided. This same mechanism was adopted for controlling air flow and mixing at the fire, but placed sufficiently high to permit the rapid cooling above the fire observed by Carroll [1977] in plumes from backing fires. The importance of the gas phase velocity profile entering the fire was shown by Wichman, et al. [1982] for thermally thick fuels (downward heat conduction important), although the importance for thermally thin fuels was not as well developed. The results of de Ris [1969] for spread of a diffusion flame in opposed flow are independent of the approach air velocity for thermally thin fuels, at least with oxygen concentrations similar to ambient air where the reaction rates may be considered infinite in comparison to the heat transfer. The observation by Mobley [1976] that the spread rate of backing fires in thin fuel layers is less sensitive to air velocity is consistent with these results.

All of the previous work involving wind tunnel studies of flame spread rate in free burning fires used stationary fuel beds with moving flame fronts. In the case of Fleeter, et al. [1984], this required following the fire with the moving ceiling in order to maintain the conditions of the semi-open channel design. For the purposes of sampling the emissions from spreading fires, the use of stationary fuel beds requires extremely long combustion test sections to permit burns of sufficient duration. The concept employed here was to translate the fuel bed relative to the tunnel floor. By moving the fuel bed at the fire propagation velocity, the flame could be held stationary in space. In principle, a fire could be sustained indefinitely with this approach. The adjustable ceiling also need not be moved once the position of the fire has been established. By fixing the position of the flame, sampling instruments could also be fixed without the need to follow the fire as occurs in the field or when the fuel bed is stationary. Monitoring the speed of the fuel bed when holding the flame stationary also provides a means of recording the fire propagation velocity, and this can be done mechanically by sensing the speed of the conveyors used to translate the bed. The concept of translating the fuel bed was later seen to be similar to the approach used by Emmons and Shen [1971] to monitor the velocity of fire spread in paper arrays. The major difficulty arising from the translation of the bed is the need to configure the bed so that the structure remains essentially intact during transport, and thus an accurate simulation of the fuel bed structure occurring in the field becomes more difficult. The structure used to convey the fuel also needs to provide minimum quench surface so as not to unduly influence the emission of volatile organics. Fuel bed structure is not the only problem occurring in the simulation of the field conditions. The wind profile and turbulence characteristics are also problematical. In fact, complete simulation of the

atmospheric boundary layer in a wind tunnel can not be achieved. As discussed by Plate [1982] however, sufficient similarity in the lower part of the layer can be obtained to warrant use of the wind tunnel in this kind of investigation. Because scaling of the fire itself appeared undesirable from the standpoint of emissions testing, the tunnel was designed with the intent of generating a sufficiently thick boundary layer above the fuel surface with turbulence intensities of the same order as the field. As mentioned earlier, sampling was to be done from the immediate vicinity of the fire, without attempting to model plume processes. Longer term reactions can be assessed through application of results from atmospheric chemistry.

Prototype Development

To test the design approach outlined above, a small scale prototype tunnel was built and tested. A schematic of this tunnel appears in Figure 1. The purpose of constructing this tunnel was to identify flame characteristics and fire propagation velocities in spreading type fires to assist in the design of a large scale tunnel described later. This tunnel incorporated a moving floor composed of individual 1.2 m long sheet steel segments pulled along the tunnel floor from below by a center mounted drag chain conveyor. The tunnel also included a manually adjusted sliding ceiling, but no hood was installed behind the fire, and the plume expanded freely into the atmosphere. Air flow through the tunnel was supplied from a centrifugal blower driven at variable speed by a hydraulic motor. A flexible coupler connected the blower duct to the tunnel diffuser to isolate the tunnel from blower induced vibration. The flow straightening elements consisted of three screens located downstream of the diffuser section. The first screen was of mesh type with an open area of

65.5%. The latter two screens were round hole screens of 30.8 and 19.8% open area. Fuel was introduced under the diffuser and entered the tunnel on the fuel conveyor segments. A wire placed across the tunnel width at the exit of the last screen and at the base of the flow straightening section was used to trip the flow just above the fuel surface. A fourth screen of 12.7 mm (1/2 inch) hardware cloth was added as a trip fence to create a more uniform profile. The tunnel was too short to develop the boundary layer profile fully, and the results were used only for the preliminary purposes of investigating flame height, length, and angle, fire propagation velocity, and uniformity of propagation into the fuel bed across the width of the tunnel. Windows were included on either side of the tunnel to view the flame. Originally these were of Pyrex but were later replaced with a neoceram glass capable of withstanding the temperature gradient across the glass.

The drag conveyor was driven by a variable speed DC motor. The speed was adjusted to match the streamwise fire propagation velocity and maintain the fire stationary with respect to the floor. Wind velocity was adjustable up to 4 m/s at the center of the tunnel with fuel present on the floor of the tunnel. Tests conducted in this tunnel indicated fire propagation velocities of 0.5 - 1.0 m/min in rice straw at about 10% moisture content wet basis and loaded at bed densities of up to 1400 g/m^2. The spread rate was seen to be mostly insensitive to the wind speed, but was influenced by the loading rate. Uniformity of the fire across the tunnel was observed to be quite good when the fuel loading was uniform. Temperature distributions were also collected in the flame using 0.5 mm type K (chromel-alumel) thermocouples. Peak flame temperatures recorded during fires in rice straw loaded at 580 g/m^2 and with wind speeds of 1.5 m/s were in the vicinity of 750°C. This value is in agreement with that

reported for natural fires [Chandler, et al., 1983] at the flame depth of 38 cm observed in the tunnel.

During this phase, studies were also made of the frequency distribution of wind speed in the field. Three-cup type anemometers were set up at 0.5 and 2.0 m elevations to record wind speed in a rice field near Woodland, California and monitored throughout the months of September and October, 1987, the months corresponding to the time when rice straw is typically burned. This study was conducted to determine the maximum wind speed to be used in designing the large scale tunnel. As shown by Figure 2, at 2.0 m elevation, the wind speed was less than 5 m/s for 95% of the time, and at 0.5 m, the wind speed was less than 2 m/s for 91% of the time. These results are similar to historical data for the same area. The maximum average speed selected for the large scale tunnel was 5 m/s.

Large Scale Tunnel Development

To simulate both spreading and pile type fires, a larger wind tunnel was designed. This tunnel incorporated many of the elements of the prototype tunnel, including the capability to translate a fuel bed so as to maintain the flame stationary in space. In addition, a hood was added above the combustion test section of the tunnel to channel the combustion products through a sampling zone. The mechanism employed to translate the fuel bed was modified, however, to reduce heat transfer to the conveyor, and to make fuel loading easier at this larger scale. The exterior design of the tunnel appears in figure 3, and a photograph of the completed tunnel is included as figure 4.

The width of the tunnel was selected to reduce the thermal dissipation at the walls to a reasonable fraction of the estimated energy release rate of the fire. Consideration was also given to the blower capacity required to reach the intended maximum wind velocity of 5 m/s, the ability to maintain a uniform fire profile across the width of the tunnel, and the physical strength requirements of the conveyor elements supporting the fuel across the width of the tunnel. Using the results of the prototype studies, the transverse thermal energy loss from the flame adjacent to the walls in a wind of 2.5 m/s and a loading rate similar to that of rice straw in the field was estimated to be approximately 17.5 kW. From the heating value of the fuel and the heating value of the residual char following the fire, the fireline intensity (energy released per unit width of fire) was estimated to be 130 kW/m. As the width of the tunnel increases, the fractional wall dissipation rate (the ratio of the wall loss to the energy release of the fire) declines in the manner shown in figure 5. There is a rapid decline in the wall dissipation rate up to 1 m width. The incremental improvement is reduced past this point. An increase in width from 1.5 to 2.0 m, for example, results in a decline of only 2% in the wall dissipation rate, but requires an increase of 33% in blower capacity to match the wind velocity. The final width was selected as 1.2 m which matched standard materials and provided a wall thermal dissipation rate of approximately 10% under the assumptions made. As indicated by Carrier, et al. [1984], boundary layers on the walls create non-uniform velocity distributions in the transverse direction. In heading fires where the fire propagation velocity depends directly on the wind velocity, wall boundary layers would reduce the effective width of the tunnel under uniform flow. In backing fires where the fire propagation velocity is thought to be less sensitive to the wind velocity, the presence of wall boundary layers is expected to have less of an

effect on the uniformity of the fire. In addition to these considerations, the tunnel width needed be large enough to accommodate full scale fuel particles in the case of spreading fires in cereal crop residues. The problems inherent in attempting to scale these particles, configure the fuel bed appropriately and convey it into the combustion test section made fuel scaling an undesirable alternative.

The tunnel consists of three principal sections: the flow development section, the combustion test section, and the stack sampling section. The entire tunnel extends nearly 26 m in length and stands about 10 m high. The tunnel is a forced draft open circuit type, using a 45 kW centrifugal blower capable of generating an average 5 m/s wind speed approaching the fire in the combustion test section.

The flow development section consists of the blower, flow straightening elements, and the primary fuel feed conveyor used when testing spreading type fires. Fuel is loaded onto the primary conveyor ahead of the blower, and passes beneath the blower, diffuser, and flow straightening elements before entering the air stream 10 m upstream from the combustion test section. The primary fuel conveyor consists of a continuous flexible solid belt 36.5 m long. The belt travels along the inner floor of the flow development section on its delivery pass, and returns on the outside below the tunnel. Fuel can be loaded continuously onto the belt as the experiment proceeds. The centrifugal blower is of fixed velocity, but has variable dampers at the inlet and outlet to adjust the air flowrate. The blower is connected to the diffuser by a flexible coupling to reduce transmission of vibration from the blower to the tunnel structure. Flow straightening is done with five screens located downstream of

the diffuser. Two 40 mesh stainless screens are followed by three 60 mesh stainless screens. Just following the last screen, the fuel enters the flow development section. In the tests described here, the ceiling was not expanded to relieve the horizontal pressure gradient, and a full simulation of the boundary layer was not attempted. This remains a future option, but the error associated with this is expected to be small. At a distance of 2.4 m upstream of the combustion test section, a wire mesh fence was installed to trip the flow shortly ahead of the fire.

The combustion test section extends 7.3 m in length. The configuration of the conveyors, floor, and ash accumulation bin are shown in figure 6. At the entrance to the combustion test section, the fuel is transferred from the primary conveyor to a stainless rod conveyor consisting of 12.7 mm diameter stainless tubes spaced every 100 mm along the tunnel and connected at the ends to continuous roller chains. The floor of the combustion test section consists of porous refractory brick which can be wetted to provide a moist surface below the fuel. The brick was placed in stainless pans connected to a manifold supplying water to saturate the brick. The brick has a specific gravity of 1.64 and is intended to remain wet in the presence of a flame, as in the case of a flame moving across a saturated soil surface.

Just above the brick and 150 mm below the rod conveyor is a third conveyor of 3 mm stainless mesh screen. This conveyor is used to convey any fines which drop through the rod conveyor downstream so that they will not serve as a source of ignition to incoming fuel. All three conveyors are driven at the same linear velocity by a variable speed DC motor regulated to match the fire propagation velocity. The rod and mesh conveyors also return on the

outside of the tunnel, and are cooled to near ambient before they enter the tunnel. An ash collection bin is located at the discharge end of the conveyors to receive and accumulate residual char as a test proceeds. This bin is sealed so as to reduce air intrusion or loss of char. A total of 25 windows of neoceram glass (Nippon Electric Glass Company) are located on the walls of the tunnel, 12 on each side and one in the end wall of the tunnel. These windows permit viewing of the flame. Each window is 508 mm wide, 660 mm high, and 5 mm thick. During operation, the flame is held on the window surfaces, rather than the sheet steel surfaces making up the remainder of the tunnel wall. Each window is held against a silicon gasket by a spring loaded frame to allow the windows to expand upon heating, although this glass is reported to have zero thermal expansion at 800°C. The windows have not failed under thermal-mechanical stress generated by operating with the flame held on the glass. The lower six windows on each side of the tunnel are installed on three doors, hinged at the top, which may be opened for inspection purposes. The doors are also designed to be opened when conducting pile fires under no wind conditions when air should be drawn from around the fuel bed. An adjustable ceiling can be extended into the combustion test section at a height of 1.23 m above the rod conveyor. A water manifold was installed at the entrance to the combustion test section to extinguish any uncontrolled fires approaching the flow development section. All materials used in the test section were thoroughly washed to remove any grease and oils which could volatilize during heating from the fire. Also, a number of preliminary tests were run in the tunnel prior to the actual acceptance tests described below.

At a height of 3.7 m above the fuel bed the combustion test section begins to narrow into the stack sampling section. Sampling ports are located

at two levels in the stack. The first level is in a section of duct 2.4 m long extending 1.2 m upwards from the initial transition. Above this is another transition leading into the second level sampling area situated in the vent stack of 1.2 m square cross section. This second level is the principal sampling area and is situated nearly 8 m above the fuel bed. Windows are also provided at both levels to view the sampling instruments and the conditions of the exhaust. A ladder and catwalks provide operator access to the sampling ports.

Flow and Fire Characterization

Investigations of the velocity profiles and turbulence intensities generated at the end of the flow development section and in the stack at the second level sampling position under cold conditions were conducted by traversing the flow in these regions with a single element hot film anemometer. The anemometer output was connected to a high speed data acquisition system. The velocity was sampled at 140 μs intervals (7,143 Hz). Long term averages were collected over a period of at least one minute in each position of the traverse. Turbulence intensities at each point were computed from 15,000 data points representing durations of approximately two seconds according to:

$$I_1 = \frac{(\overline{u'u'})0.5}{u} = \frac{\sigma_u}{u} \qquad \{2\}$$

where I_1 is the turbulence intensity normalized to the mean velocity, u, in the streamwise direction, u' is the velocity fluctuation from the mean, $(\overline{u'u'})0.5$ is the root mean square of the fluctuation, i.e., the standard deviation, σ_u.

Velocity profiles and turbulence intensities for a mean velocity of 2.35 m/s are shown in figures 7 through 10. The duct Reynolds number at this velocity was 1.9×10^5. Figures 7 and 8 show the velocity profiles through the center of the tunnel in the vertical and horizontal directions. These profiles were determined in the combustion test section with the ceiling extended and approximately 250 mm upstream from the edge of the ceiling. These data were collected without a fire in the tunnel, but with a bed of rice straw (600 g/m^2) extending the full length of the flow development section and into the combustion test section. Figures 9 and 10 are velocity profiles through the center of the stack at the second level sampling area in the transverse (east-west) and longitudinal (north-south) directions. These were also taken without a fire in the tunnel. The vertical profile at the entrance to the fire (Fig. 7) shows the boundary layer extending some 35 to 40 cm above the fuel surface as well as a boundary layer of some 10 to 15 cm thickness developed on the ceiling of the tunnel. A comparison of the boundary layer over the fuel to that computed for a natural grass surface estimated to be of similar roughness to the field shows similarity up to about 35 cm depth (figure 11). The latter profile was computed from a logarithmic law of the wall [Sutton, 1960]:

$$u = \frac{u*}{k} \ln \left(\frac{z-d_o}{z_o} \right) \qquad \{3\}$$

where u is the wind velocity (m/s) at elevation z (m) normal to the surface, k is von Karman's constant, here taken numerically equal to 0.4, $u*$ is the friction velocity (m/s), d_o is the zero plane displacement (m), and z_o is the surface roughness parameter. Values used in developing figure 11 were $u* =$

0.32, z_o = 0.02, and d_o = 0, and were adapted from Sutton [1960] for a grass of 5 cm height. The 35 cm thickness corresponds roughly to the flame height of a field backing fire in rice straw as shown later. Plate [1982] has shown that equation {3} is valid with roughness height z_o which depends only on the geometry of the roughness elements of the surface, and is independent of any Reynolds number for roughness Reynolds numbers $u*z_o/\nu > 5$, which is the situation of figure 11. The wind profile above 35 cm in figure 11 shows that there is not good development above this level, and additional roughness should be tried in the future to increase the depth.

The velocity profile across the horizontal direction at the inlet is fairly uniform (Figure 8) except for the boundary layers of some 20 cm depth at the wall. Such boundary layers do not appear in the stack, and in fact the stack velocity profiles are uniform very close to the walls (Figures 9 and 10). Conditions of uniformity for sampling the stack appear to be satisfactory at least at the second level sampling station.

As Cermak [1971] and Plate [1982] have stipulated, exact simulation of the atmospheric boundary layer does not appear possible in wind tunnels. However, many comparisons have shown good similarity despite relaxation of requirements for exact simulation. Undistorted scaling would require matching of the Rossby, Richardson, Reynolds, Prandtl, and Eckert numbers (Cermak, 1975). For the surface layer of the atmosphere, the region of interest here, the Rossby number, which describes the Coriolis effect, is of lesser importance and cannot at any rate be matched in the wind tunnel. By using air as the oxidizer in the wind tunnel, Prandtl number similarity is automatically satisfied. The Eckert number cannot be matched if the bulk

Richardson number is matched, and is of lesser importance at low speeds [Plate, 1982]. The Richardson number can be matched by adding surface heat flux, but this is unnecessary for the purpose here. The Reynolds number of the atmosphere is generally so large that its influence on model similarity is negligible (Panofsky and Dutton, 1984). For rough boundaries, no limitations on simulation generally appear (Cermak, 1975). The Reynolds number here is, at any rate, sufficiently high ($>10^5$ at 2 m/s) to ensure fully turbulent flow in the tunnel, and as indicated above, to permit the use of equation {3}.

Of primary importance is to attempt to match the gross velocity profile and the turbulence characteristics of the flow within the immersion depth of the flame, which Plate [1982] has indicated are the two conditions necessary to satisfy similarity for the conditions here. By matching turbulence intensities, the root mean square fluctuations are constant between model and prototype at the same wind speed. It also appears that if the mean velocity profiles are matched, the scaling frequencies are matched as well (Plate, 1982). Wichman [1983] and Wichman et al. [1982] have demonstrated the dependence of the fire propagation characteristics on the velocity profile of the air entering the fire. In fact, Wichman [1983] has used this result to relate experiments conducted under different external flow conditions which yield similar flame spread rates. Comparing fires conducted under forced convection in wind tunnels with open flames in a free convection boundary, he finds the results to be identical based on velocity profile similarity over nearly an order of magnitude change in air velocity.

As already noted, the velocity profile within the lower 35 cm of the wind tunnel matches reasonably well a logarithmic profile computed for the

atmosphere. The logarithmic profile can be developed on the basis of Monin-Obukhov similarity theory and from K theory. Without surface heat flux, the flow simulates a wind profile in neutral air where mechanical turbulence dominates. The derivation appears elsewhere, and will not be repeated in its entirety here (see for example, Lumley and Panofsky, 1964; Panofsky and Dutton, 1984; Pasquill, 1974; Nieuwstadt and van Dop, 1982; Plate, 1982). The momentum flux is formulated as

$$\tau = K_m \rho \frac{\partial u}{\partial z} \qquad \{4\}$$

where τ is the Reynolds stress component in the streamwise direction, K_m is the exchange coefficient for momentum, or the eddy diffusivity, and ρ is the density. With K_m proportional to a product of eddy size and eddy velocity, eddy size proportional to height z, and eddy velocity proportional to the friction velocity u*,

$$K_m = ku*z \qquad \{5\}$$

with the requirement that $K_m = ku*z_o$ at the surface where z_o, the roughness length, represents the eddy size at the surface. Substitution of {5} into {4} with the definition of the friction velocity ($u* = [\tau/\rho]^{1/2}$) yields equation {3} upon integration with the exception of the zero plane displacement, d_o, sometimes used to account for the height of the roughness elements. Panofsky and Dutton [1984] have suggested an appropriate model scaling can be done on the basis of a Reynolds number Re = Lu/zu* where L is the Monin-Obukhov length scale. Under neutral conditions, u/u* depends only on z/z_o . Since z

and L are scaled by the same length, Reynolds number similarity will occur if z_o is scaled by the same length scale. For a direct simulation, this implies that z_o should be matched between the wind tunnel and the field.

The analysis may also be used to estimate the magnitude of the turbulence intensities. The standard deviations of the wind components in all three directions have been shown to be proportional to the friction velocity under neutral conditions in the form (Panofsky and Dutton, 1984):

$$\sigma_i = A_i \, u* \qquad \{6\}$$

where A_i is a constant depending on the direction, i. The value of A_u in the streamwise direction (u) has been shown to be very close to 2.5 (McBean, 1971; Lumley and Panofsky, 1964; Panofsky and Dutton, 1984), which in combination with equation {3} results in the turbulence intensity in this direction being related to the height z as:

$$\frac{\sigma_u}{u} = \frac{1}{\ln(z/z_o)} \qquad \{7\}$$

For z_o = 0.02 m (Fig. 11), this yields estimated turbulence intensities of the magnitude shown in Fig. 7. Estimates of intensities are about twice as large as those measured in the tunnel, but decrease upwards from the surface in the same manner. Turbulence intensities in the range of both the estimates of equation {7} and those measured in the wind tunnel (40% just above the fuel surface decreasing to about 10% at 60 cm height) have been reported in the literature. Plate [1982] summarizes field data for z_o = 0.05 to 0.5

m which are nearly identical to those measured in the wind tunnel. Cionco [1972] measured horizontal turbulent intensities of 30 to 100% in the region immediately above a crop canopy . Maitani [1979] measured turbulence intensities over various surfaces and found values of 40 to 120% in the region just above plant canopies. The turbulence intensity decreased with height in a manner similar to that measured here. Maitani concluded that his data showed $\sigma_u/u*$ to be invariant with height in a manner consistent with equation {6}. Ohtou, et al. [1983] consistently measured turbulence intensities of about 50% at an elevation of 65 cm above a rice crop. Ohtaki [1980] measured turbulence intensities of about 40% at 80 cm above a rice crop.

Seginer, et al. [1976] conducted wind tunnel experiments of flow over simulated crop canopies. The wind tunnel had a working section of 1.8 m in width and 0.6 m in height. Turbulence generating grids were used to trip the flow ahead of the model canopy. Turbulence intensities were essentially constant in the canopy, and decreased from 45% at canopy height (20 cm) to 12% at 50 cm height before entering the ceiling boundary layer. Similar results were obtained by Finnigan and Mulhearn [1978] who modelled waving crops in a wind tunnel. Turbulence intensities were approximately 40% immediately above the crop and decreased upwards to values approaching 10%, similar to measured values here. A wind tunnel study of the wind induced loads on ground vehicles by Baker and Gawthorpe [1983] used a flow with a turbulence intensity of about 20% to simulate the atmospheric level. These results are not entirely consistent, but indicate that existing turbulent intensities are of the right order, but perhaps low by as much as a factor of about 2.

While the hot film anemometer used here did not permit measurement of the vertical component of turbulence intensity, estimates may be made on the basis of equation {6}. Verification should be performed in future work. Panofsky and Dutton [1984] report that A_W (in the vertical direction) is on the order of 1.25, implying that σ_w is approximately 0.40 m/s for the conditions measured. This value is in good agreement with values reported by Ohtaki [1980] and Ohtou, et al. [1983] in flow over a rice crop. The vertical component is important for upward transport as the eddy diffusivity is proportional to $\sigma_w{}^2$. Pasquill [1974], for example, presents a model for the diffusion of material injected into the atmosphere from ground level along a line source. The concentration gradients are solved using an analogy to momentum transfer where the value of the exchange coefficient is taken equivalent to K_m.

The influence of the velocity profile on the fire spread velocity has already been noted above. Also of concern is the effect on flame extinction, as this has potential importance in the determination of the emissions from the fire. In most studies of flame spread, the kinetics are assumed to be fast, and heat and mass transfer limiting. de Ris [1969] made this assumption in his model. He also pointed out conditions under which this assumption would not be valid. Limiting cases appear when the concentration of oxidizer in the gas stream is low, and when the gas velocity is sufficiently high to blow out the flame. Later studies have dealt with finite rate solid and gas phase kinetics and flame extinction in more detail (Williams, 1985). Frey and T'ien [1979] and Altenkirch, et al. [1980] have conducted studies which take into account heat and mass transfer in the propagation of the flame and the chemical kinetics of the solid phase pyrolysis and gas phase combustion. Altenkirch's analysis also

includes a buoyancy term, such as that suggested in a comment by de Ris [1969]. Altenkirch et al. correlated their own data and that of Frey and T'ien against a reduced Damkohler number to determine when the fast kinetics case would apply. The reduced Damkohler number, D, is of the form:

$$D = \frac{B\,\lambda\, m_{ox}}{W_{ox}\, c_p (v g Q m_{ox}/T_\infty r c_p)^{2/3}} \left(\frac{T'^2_f}{T'_a}\right)^3 \exp\left(-\frac{T'_a}{T'_f}\right) \qquad \{8\}$$

$$T'_a = \frac{E}{R(Q m_{ox}/r c_p)} \qquad \{9\}$$

$$T'_f = \frac{T_f}{Q m_{ox}/r c_p} \qquad \{10\}$$

where B is a preexponential factor for the gas phase reaction, λ is the thermal conductivity of the gas, m_{ox} is the oxygen mass fraction in the ambient fluid, W_{ox} is the molecular weight of oxygen, c_p is the thermal capacity of the gas, ν is the kinematic viscosity of the gas, g is the gravitational acceleration, Q is the enthalpy of the reaction for gas phase combustion, T_∞ is the absolute temperature of the ambient fluid, T_f is the flame temperature, and r is the mass of oxygen needed to consume a unit mass of fuel. R is the universal gas constant and E is the activation energy. T'_a is a dimensionless activation "temperature". Altenkirch found D to correlate well with a dimensionless spread rate:

$$V = \frac{\rho_s V_{Ft}}{\mu} \frac{c_s}{\sqrt{2} c_p} \frac{(T_v - T_\infty)}{(T_f - T_v)} \qquad \{11\}$$

where ρ_S is the density of the solid, V_F is the fire spread rate, t is the half thickness of the fuel element, μ is the fluid viscosity, c_S is the thermal capacity of the solid, and T_V is a vaporization temperature for the solid. V approaches 1.0 at high Damkohler number, which is the fast kinetics limit of de Ris. Similar Damkohler number correlations have been used by Frey and T'ien [1979], Wichman et al. [1982], and Carrier et al. [1984]. Using this analysis, parameter data from Altenkirch et al., and the conditions for the rice straw tests described later with air, the value of D is on the order of 10^3, which is above the extinction limit of Altenkirch and yields a value of V near 1.0 according to Altenkirch's correlation. This implies that the gas phase kinetics are not limiting. The spread rate predicted by equation {11}, assuming the fuel bed tested is an assembly of thermally thin fuel elements, is of the same order as experiment, but radiation heat transfer within the bed has not been treated fully, yet is of some considerable importance for fire spread. Peclet number ratio similarity of the type employed by Wichman et al. [1982] also suggests that gas phase heat conduction plays an important role in the rate of propagation of the fire through the fuel bed. Carrier et al. [1984] utilized both the so-called first and second Damkohler numbers in their dimensional analysis, but discarded the first Damkohler number because they considered forced-convective extinction of combustion to be of no interest aside from delineating the domains of flame propagation. Carrier's analysis considered wind-aided, or heading, fires predominantly. At very high velocities, it may be possible to blow out the fire in a manner similar to that suggested by de Ris, but this has not been possible so far with the maximum wind speed obtainable in the tunnel and the fuel conditions tested.

Tests were also conducted to determine if the time-temperature relationships of fires in the field are adequately matched in the tunnel. Field data were obtained for both backing and heading fires to assess the quality of some existing literature pertaining to this subject. Field data on the backing fires were also compared against wind tunnel data obtained for four separate configurations in the tunnel.

Results of two field tests in rice straw are shown in figures 12 and 13. Temperature data were obtained by positioning eleven 0.5 mm diameter type K thermocouples in two vertical arrays horizontally separated by 0.95 m within the field plot to be burned. Nine thermocouples were placed in the upstream array. The first thermocouple was located just under the soil surface, with additional thermocouples at 76, 152, 279, 318, 356, 508, 813 and 1397 mm above the soil surface. The tests were conducted in rice straw spread behind the harvester in the conventional manner and situated on the top of the uncut portion of the plant stems (stubble). Straw moisture ranged from 5 to 8.5% wet basis, at a loading rate of 576 to 612 g/m^2 dry basis. Thermocouples at 279, 318, and 356 mm were located at the lower straw layer surface, in the interior of the straw layer, and at the surface of the straw layer respectively. Two thermocouples located in the second array were positioned at 279 and 356 mm above the soil, again at the two surfaces of the straw layer. The fires were burned either in direct opposition to the wind, or directly with the wind. The thermocouples were sampled at 4 s intervals, which was sufficient to capture the duration of the burn as the fire moved past the thermocouples, and generally adequate to obtain peak temperatures possible with this system. For these tests, the wind velocity ranged from 1 to 2 m/s at 0.5 to 0.6 m elevation.

Results from the two upper surface thermocouples from both arrays at 356 mm elevation are shown in figure 12 (a) for a backing fire and 12 (b) for a heading fire. The spreading velocity for the backing fire was 0.95 m/min, while that for the heading fire was 3.6 m/min. Contour plots of temperature as measured by the thermocouples reveal the difference in flame profile, and are shown in figure 13 (a) for the backing fire and figure 13 (b) for the heading fire. The temperature has been plotted against time and elevation, but the time axis can be used as an indication of the horizontal flame position, with the fire propagating in the direction of zero time. In these plots, the elevation in the straw layer has been greatly exaggerated. The backing fire has a much lower flame height than the heading fire, and is angled in the opposite direction. The time scales show that the backing fire has a length of 0.75 - 0.95 m, while the heading fire has a length of 2.0 - 2.4 m, where the length includes cooling to 100°C. This implies considerable fuel involvement behind the leading edge of the fire in the case of the heading fire. The period of elevated temperature at the fuel surface lasts about 60 s in the case of the backing fire, and about 40 seconds in the case of the heading fire. Measured peak temperatures in both cases are 800 - 900°C. Results from the backing fire shown here do not reproduce the data of Goss and Miller [1973], which imply a longer duration for the backing fire. The data of Goss and Miller are not well described, but may represent the fire propagation into windrowed straw with a much heavier loading rate and deeper fuel layer. Straw is no longer permitted to be burned in this manner in California.

Comparable tests in the wind tunnel conducted in backing mode show similar trends in temperature and duration. Results of temperature measurements made at the fuel surface are included in figures 14 (a - d) for

the four different configurations tested. Results from a test with the fuel carried on the open rod conveyor and the ceiling extended to the leading edge of the fire (open bed, ceiling following flame) are shown in figure 14 (a). The peak temperature is about 800°C, and the duration is about 60 s. The results for the case where a steel sheet was inserted just beneath the rod conveyor (closed bed) with the ceiling extended are shown in figure 14 (b). Peak temperature is about 880 °C, with a duration of about 40 s. Results for the two configurations similar to figures 14 (a) and (b) but without the ceiling extended are shown in figures 14 (c) and 14 (d). With the thermocouples located about 2 m downstream of the combustion section inlet, there was deceleration of the inlet air, so that the flames were much more erect in these two latter cases. With the open bed, the peak temperature is again about 800°C, but the duration is somewhat shorter at about 40 s. When the bed is closed from below, the peak temperature was also about 800°C, but the duration extended to about 60 s. Some of the differences may be due to unavoidable irregularities is fuel distribution and loading. All these show reasonable correspondence to the field data. Spreading velocities for the open bed configurations were 0.93 to 0.96 m/min, while the closed bed configurations yielded spreading velocities of 0.64 to 0.68 m/min. These limited tests are insufficient to confirm matching to the field conditions for any one configuration. Additional observations will need to be made to compare emissions from the different configurations.

Heading fires would be more difficult to conduct in the tunnel, although possible with modification to the fuel loading arrangement. In heavy fuels at higher wind speeds, the fire propagation rates and flame heights would be sufficiently high to warrant concern over the effects of the tunnel on the fire

dynamics. Because heading fires are not permitted for agricultural fuels, provisions for this type of testing were not deemed relevant.

Emissions Testing

Two experiments were conducted to determine if repeatable data could be obtained on emissions from fires conducted under similar conditions of wind speed, fuel type, fuel loading, fuel moisture, air temperature and relative humidity, and moisture status of the floor. Experiments on 1 September 1988 and 7 September 1988 were conducted using rice straw at a mean wind speed of 2.35 m/s and a loading rate to match that of the field at 7% moisture, or approximately 600 g/m^2. Both tests were conducted in the mode of figure 14 (a), that is, with the bed open from underneath, and the ceiling advanced to the leading edge of the fire. Each test was designed to accumulate information on:

Fuel consumption
Fuel proximate analysis
Fuel higher heating value
Fuel ultimate elemental analysis

Residual char yield
Residual char proximate analysis
Residual char higher heating value
Residual char ultimate elemental analysis

Inlet air temperature
Inlet air relative humidity
Pressure drop across flow straightening elements
Exhaust gas temperature at sampling station
Exhaust gas velocity at sampling station
Temperatures in and above the flame

Particulate matter concentration and size distribution
Exhaust gas concentrations for:
CO_2, CO, NO_2, NO, SO_2, CH_4, C_2H_2, C_2H_4, C_2H_6, C_6H_6

In sampling for benzene concentrations, attempts were made to identify other organic compounds as well.

The sampling train used in conducting these experiments is illustrated in Figure 15. Samples were drawn from the second level sampling station through one of the ports in the sidewall of the stack. The sample was removed isokinetically with a stainless steel probe, 9.5 mm in diameter, located in the center of the stack. The end of the probe was bent and cut 90° from the probe axis, such that it faced into the exhaust stream. The probe flowrate was matched to the stack velocity measured by a hot film anemometer positioned near the probe. The probe was connected to a 25 mm i.d. heated line of flexible stainless steel tubing lined with teflon and wrapped with heating tape. The line was controlled to within ±2°C by a temperature controller using an imbedded type K thermocouple. The sample line was fed to a heated chamber made of aluminum having a volume of 2.5 L from which the samples were drawn via stainless steel pipe connectors tapped into the wall. An insulated and heated box enclosed the filters and cascade impactors. The interior temperature of the box was monitored with thermocouples and maintained at a constant temperature of 100°C. During the two tests on 1 September and 7 September, the stack gas temperature was about 50°C.

Two cascade impactors were used. The first was a high temperature, high pressure (HTHP) impactor (Model 02-300, In-Tox Products, Albuquerque, NM) operated at 13.3 L/min average flow. This impactor was constructed of stainless steel and used wire gaskets made of brass or gold between stages to seal the impactor by crushing the wire. It is capable of using any thin

collection substrate. For the tests reported here, Gelman Micro-Quartz filters were used (Part #66089 47 mm, Gelman Sciences Inc., Ann Arbor, MI). The filters were hand cut to 37 mm diameter for all stages except the final filter stage which was left at 47 mm diameter.

The other was a Sierra Impactor (Model 220K, Sierra Instruments, Carmel Valley, CA) and was operated with an average flowrate of 21 L/min. The last two stages of this eight stage impactor were not used because of the high backpressure and plugging problems in these stages. The impactor is a rectangular slot jet type using glass fiber filter paper specially cut to fit the stages (part #0-220-GF). The impactor was sealed with Viton "O"-rings compressed by two bolts. The back-up filter was a glass fiber filter (Part #61631 type A-E 47 mm, Gelman Sciences Inc., Ann Arbor, MI).

The flow was controlled with a valve and a critical orifice behind each impactor. The pressure after the impactors was monitored using a Magnehelic pressure gage so that pressure drop across the impactors could be observed. Tests were run long enough to load the filters without decreasing the flowrate substantially.

Two other samples were drawn from the sample chamber. One stream was used for volatile organics analysis on sorbent tubes. The other was used for gas analysis. Each line was filtered through a Micro-Quartz filter. Flow through each sorbent tube was pulled by a timed flow controller and pump at a rate of 100 mL/min for a period of ten minutes yielding a total flow of 1 L. The sorbent tubes used were 6 mm o.d. packed with 50 mm (2 inches) of Tenax-TA 20x30 mesh and 38 mm (1.5 inches) of Ambersorb XE-340 (tubes supplied by

T.R. Associates, Lewisburg, PA). The tube was placed immediately after the heated box and connected with a soft graphite ferrule on teflon tubing. The gas sample line was connected via 6.4 mm teflon tubing to a diaphragm pump and an ice bath impinger train before descending to ground level. Samples were pulled from this line for each of the NO_X, SO_2, and CO analyzers located in an instrument trailer next to the tunnel (figure 4). All other equipment was located on the catwalk at the second level sampling station. After each test, the sample train was lowered to ground level, allowed to cool, the impactors and tubes extracted from the sample system and taken to the laboratory for analysis. Particulate filters were allowed to equilibrate and weighed on an electrobalance to obtain mass fraction. Sorbent tubes were analyzed by GC-MS. Adsorbed materials were purged from the trap and onto the GC by flowing helium through the tube while heating in a thermal desorber. For quantifying benzene concentration, a standard gas mixture was drawn through a blank tube and analyzed in the same manner as the sample tubes. In an earlier test, tedlar bag samples had also been collected and analyzed against the standard using a GC-PID. These two methods were found to give comparable results. Standards for other compounds were not run, but qualitative analyses were attempted for materials identified by the library program of the GC-MS.

The NO_X and SO_2 analyzers (Model 8840 and 8850, Monitor Labs, San Diego, CA) were supplied with sample from a source pump and dilution module (Monitor Labs Model 8730) which diluted the sample 20 to 1 with purified ("zero") air by means of a critical orifice. Sample dilution was specified on the basis of results from the prototype tunnel which indicated levels within the source range of the instruments, which are designed as ambient monitors.

Carbon monoxide was first monitored using an electrochemical polargraphic analyzer but was later monitored with an infrared gas analyzer (Anarad AR-500). All three instruments had been calibrated by Air Resources Board staff prior to use. Grab samples were collected in glass bulbs at regular intervals throughout each test. These were returned to the laboratory and analyzed by GC/TCD for CO_2 and low molecular weight hydrocarbons. Ambient air background samples were also collected and analyzed.

Other instrumentation included various transducers for monitoring the conditions of the test, and the data acquisition system to read, process, and store the data. Inlet air temperature and relative humidity were monitored downstream of the blower by a thermistor and polymeric grid type humidity sensor (Campbell Scientific Model 207, Logan, UT). Pressure differential across the screens was monitored with a strain-gage type pressure transducer. Temperatures in the flame, in the stack, and at the outlet of the impingers were monitored with type K and type T thermocouples. Velocity in the stack was monitored using a hot film air velocity sensor (Kurz Instruments, Carmel Valley, CA) capable of withstanding the particulate load in the gas stream. All sensors except the velocity transducer were connected to an electronic datalogger (Campbell Scientific Model CR21X, Logan, UT) which was serially interfaced to a microcomputer (IBM PC-AT) running a custom data acquisition program to store the data on disk and output results to the screen in either text or graphics mode. Outputs from the NO_X, SO_2, and CO analyzers were also connected to the datalogger and computer. Results were written to disk every three seconds throughout the test. Five 0.5 mm type K thermocouples were suspended from the leading edge of the adjustable ceiling into the flame. These were labeled numbers 10 through 14 with the beads positioned at 44 (No.

14), 70 (No. 13), 127 (No. 12), 146 (No. 11), and 216 (No. 10) mm above the surface of the rod conveyor.

Combustion tests were started by loading fuel onto the primary fuel belt and stainless rod conveyor up to the point of ignition at the third window 3 m downstream of the entrance to the combustion test section. To obtain the loading rate desired, sections of the primary fuel belt of area 2 m^2 were marked and loaded with a weighed amount of fuel. The fuel was then spread as uniformly as possible over the surface of the belt. This was done as the belt was continuously moved into the flow development section until the conveyors were fully loaded. Both tests were run with approximately 600 g/m^2 of fuel and with a dry floor in the tunnel. In operation, some of the fine material separated at the transfer point between the primary fuel conveyor and the rod conveyor. This material was collected and weighed. The actual loading rate was somewhat less than 600 g/m^2 due to the separation of these fines. Samples of the fuel were collected as the belt was loaded, and continued to be taken as the experiment progressed. The ceiling was extended to just upstream of the ignition point. All gas analyzers were turned on at least an hour before ignition, and were checked for zero and span. The computer data acquisition system was started and all sensors checked. The stack gas sampling equipment including cascade impactors, impingers, sample pumps, and controls, were lifted to the second level sampling station. The probe, thermocouple, and anemometer were inserted into the stack. The heated sample chamber was brought into equilibrium at 100°C. Gas sample lines were connected to the on-line gas analyzers, and glass sample bulbs prepared to collect grab samples of the gas. When all sampling apparatus had been stabilized, the blower was started at the flowrate set by the inlet and outlet dampers to match the desired

mean wind speed. The fuel was ignited quickly across its leading edge with a propane flame to establish the fire. At the same time the fuel was ignited, the sample pumps were started to draw effluent through the emissions sampling system. As the flame began to advance, the DC motor controlling the conveyor travel was started and manually adjusted to match the natural fire propagation velocity. On both tests, the motor speed did not require further adjustment after the initial setting because the fire propagation rate remained quite uniform. The fire propagation velocity was obtained by observing the speed of the fuel conveyors, and could also be computed from the total fuel consumption and the loading rate. Both tests lasted approximately thirty minutes. The duration was adequate to load the filters of the cascade impactors, and to collect three sorbent tubes exposed to the effluent every ten minutes over the course of the test. Each test was terminated by allowing the fire to extinguish itself when all fuel on the conveyors was consumed. Following the test, the mass of residual char (which will hereafter be referred to as ash) was determined and samples collected for analysis. The material was hygroscopic and accumulated some moisture on cooling. Ultimate analyses were performed by the Microchemistry Laboratory of UC Berkeley. Proximate analyses, heating value determinations, and major gas analysis were done at the Agricultural Engineering Department of UC Davis. Particulate sample analysis was done at the Institute for Environmental Health Research (IEHR) of UC Davis. Sorbent tubes were analyzed at the Facility for Advanced Instrumentation (FAI), also at UC Davis.

The initial design of the fuel conveying system had not included the stainless mesh conveyor beneath the rod conveyor. Early tests of the system showed that burning fine material dropping through the rod conveyor could

cause ignition of new fuel entering the flame region faster than it otherwise would have ignited. In some cases this led to a planar ignition of the fuel which propagated in an uncontrolled manner not seen in the field. The addition of the lower mesh conveyor advanced the material falling through the rod conveyor at the same rate as the main body of fuel, and prevented early ignition of incoming fuel. In actual fuel beds, the separation of fines to the soil surface does in fact occur. The upper and lower conveyor system may therefore improve the fire simulation relative to a single conveyor system. By holding the flame stationary on the window, the wall temperature can increase to avoid quenching effects seen when the fire is allowed to propagate along a stationary fuel bed.

Results

Results of the fuel and ash analyses for both tests are included in Table 1. Fuel moisture was similar in both cases (6.5 and 7.3% wet basis). Results of the proximate and ultimate analyses are also similar with the exception of the concentration of sulfur and chlorine in the ash for the test of 7 September. A replicate of this sample yields a sulfur concentration of 0.07% for the fuel and 0.05% for the ash. These values appear highly variable and uncertain at this time, and require further evaluation.

Material balances and characteristics of the fire appear in Table 2. The fire propagation velocities in both tests were nearly equal at 0.96 and 0.93 m/min. This value corresponds with values reported by Mobley [1976] for backing fires in grass fuels at similar moisture, and to the velocities obtained in the field tests described above. The difference in the two values may be due

to a slightly lower loading rate and slightly higher moisture content for the test of 7 September. Total ash recovery is similar to what would be expected on the basis of the inorganic component of the fuel and ash. The amount recovered from the first test is somewhat higher than expected, and the amount from the second test is somewhat lower, but both are close to the anticipated value and are within the expected experimental error. There is some loss of ash to the floor of the tunnel which cannot be fully recovered and is lost during cleaning in preparation for the next experiment.

Inlet air conditions for both tests are shown in figure 16. Relative humidities are quite similar. The air temperature of 1 September is slightly higher, and results in a higher stack temperature compared to the test of 7 September (figure 17), although the difference is only about 5 K on average. The presence of a fire in the tunnel causes a temperature increase of 15 - 20 K above inlet at the stack. This implies a dissipation rate of approximately 80 kW of thermal energy, or half of the energy released by the fire (160 kW) determined on the basis of the difference in heating values of the fuel and ash. Roughly 20 kW is estimated to be transferred from the flame through the windows by radiation, conduction and convection. The remainder is lost to the structure of the tunnel and by cooling of the ash after deposition in the ash accumulation bin.

Fire temperatures are shown in figures 18 and 19 for thermocouple locations 10 and 14. Rapid cooling was seen to occur immediately above the reaction front (compare thermocouple 10 at 216 mm to thermocouple 14 at 44 mm). Peak flame temperatures were observed to be about 800°C.

Average concentrations of the gas phase emissions observed during each test are listed in Table 2. Total NO_x emissions averaged 3.65 ppm, of which 80% was in the form of NO. As shown by the material balance for nitrogen, the concentrations of N in the ash and in the gas phase emissions of NO and NO_2 account for only 20% of the fuel nitrogen.

SO_2 emissions were extremely difficult to measure, the signal from the analyzer being only slightly above the noise level of the instrument. The values reported are uncertain, but there does not appear to be a significant quantity of SO_2 in the gas. The discrepancy in the sulfur concentrations in the ash by ultimate analysis makes it difficult to compare the closure values on sulfur, but the gas phase emission of SO_2 is likely to be well below that computed on the difference of sulfur in the fuel and the ash as reported by Darley [1979]. The low readings obtained on the SO_2 analyzer indicate that an ambient monitor should have been used because the actual concentrations are so much lower than those estimated from the fuel bound sulfur.

Carbon balances show reasonable closure levels, being 89% for the test of 1 September and 95% for the test of 7 September. The carbon balance is extremely sensitive to the concentration of CO_2 determined for the stack gas. In both cases, the mean value was determined to be 0.2% exclusive of ambient level. The difference in fuel carbon and ash carbon would yield a concentration of approximately 0.24% if all volatile carbon were converted to CO_2. Carbon concentrations of particulate materials have not yet been determined, but cannot contribute more than 0.5% to the closure.

Concentrations of CO were comparable for both tests. To confirm the values obtained, an additional test was conducted on 21 September with similar results. Other gas concentrations were not determined during this latter test.

The predominant hydrocarbon was methane at an average of 6 ppm, although the concentration measured on 7 September was half that of the value on 1 September. Concentrations of other light hydrocarbons are comparable. Ethene (ethylene) is the next highest concentration after methane.

Benzene concentrations determined from the sorbent tubes were in the range of 100 ppb. Previous tests in the tunnel with rice straw had also indicated a concentration of about 100 ppb. The analysis of benzene by trapping on the sorbent tubes was compared to grab sample analyses using tedlar bags by analyzing a standard gas with a reported concentration of 112 ppb. The sorbent tube analyzed by GC-MS yielded a concentration of 111 ppb and the bag sample analyzed by GC-PID yielded 117 ppb. The values appear to be in adequate agreement. Chromatograms from the GC-MS exhibit a large number of compounds, some of which were tentatively identified using the library of the instrument and comparing boiling points and mass spectrograms. A typical chromatogram is given in figure 20. This chromatogram was generated under a temperature program started at 40°C for four minutes and ramped at 10°C/min to 220°C and held. Tentative qualitative identification has been made for toluene, ethyl benzene, ethenyl benzene, benzaldehyde (possible artifact from tube packing), phenol (possible artifact), and napthalene. A significant amount of additional work is required to both qualitatively and quantitatively determine volatile organics emitted from the

fire. There is also some concern that quench effects could be contributing to the concentrations of volatile organics observed. Further investigation is required in this respect as well.

Particle concentrations and size distributions measured by both the Sierra and HTHP cascade impactors are given in Table 3. The HTHP impactor gave better consistency and improved fractionation compared to the Sierra. The size distributions were matched to an equivalent mass median aerodynamic diameter using a log-normal distribution with the stage efficiency least squares method [Raabe, 1968]. As a result of collecting most of the particulate on the filter stage of the Sierra impactor, the aerodynamic diameter is less than that obtained from the HTHP impactor. Total concentrations were of similar magnitude, about 9 mg/m^3. About 90% of the particles are below 4 μm in size, and 80% are less than 1 μm.

The high filter fraction on the Sierra impactor is believed to be due to stage filter material adhering to the "O"-rings during removal. This is the result of the higher temperature operation of this device than normally occurs with ambient air sampling. When a filter was removed, an attempt was made to scrape any filter material off the "O"-ring and back onto the filter, but in low mass collections this variable sample error would affect the quality of the data obtained with the Sierra impactor. The effect of any lost weight would be to skew the distribution towards the smaller particle sizes because the back-up filter does not use an "O"-ring for sealing. Future measurements should account for this effect by using different filter media and a different sealing technique.

The character of the particulate from various regions of the fire was examined by sampling the fire from a rice straw fuel conducted in the prototype tunnel. Samples were collected with a point to plane electrostatic precipitator on a carbon coated electron microscope grid. Samples from a nuclepore filter were also collected. These samples were examined under transmission and scanning electron microscopes at the Facility for Advanced Instrumentation at UC Davis. Several electron micrographs are included in figures 21 through 28. Figures 21, 22, 23, and 24 are all of samples collected directly from the pyrolysis zone of the fire within the interstitial gas phase of the fuel bed. The presence of liquid droplets containing solid material is clearly indicated. The fine nature of the particles at this stage of the fire is also seen. Flyash and soot collected in the plume behind and above the flame can be seen in figures 25 and 26. Individual particles are of the order of 100 nm in size, with larger chain aggregates formed of these smaller particles. A large flyash particle is shown in figure 26, also with aggregate material on its surface. Behind the flame in the fuel bed there generally exists an incandescent region of char oxidation. Samples collected from this region also contain primarily fine particulate with some liquid residue. The zone behind the flame has already been shown to be a source of emission, primarily from heading fires, but to some extent from backing fires as well. Observations of the tests conducted in the large scale tunnel showed that emission of particulate from this region had almost entirely ceased 4 m behind the flame. In field fires, where the fuel distribution is non-uniform, deep deposits of fuel have been observed to smolder for some time after the fire has passed. This was not observed with the uniform loadings in the tunnel. Field observations of smoldering behind the flame show it to be much more prevalent with heading fires than with backing fires.

Emission factors computed on the basis of the concentrations obtained during the two experiments of 1 September and 7 September are listed in Table 4. These are preliminary factors only, due to the nature of the conditions of the tests conducted which are only partially representative of the field conditions pertaining to rice straw burning. The results of Darley [1979] are listed for comparison. Data for particulate emissions are from the HTHP impactor only because of the filter recovery problem encountered with the high temperature operation of the Sierra impactor.

Discussion

The average emission factors compiled in Table 4 are generally consistent with those reported by Darley [1979], with some notable exceptions. Darley's particulate data is three times lower than the data from the tunnel. His NO_x data is somewhat higher, and his SO_2 data is five times higher than that obtained in the tunnel. It appears likely that the particulate emission factor reported by Darley [1979] is in fact an error, as it is not consistent with the reported value in Darley [1977] nor with the data reported by Goss and Miller [1973] who worked with Darley in developing their data. Darley [1977] reports an emission factor of 3.47 kg/t for a backing fire in 9.3% moisture rice straw conducted by burning on a 25° slope, and 4.64 kg/t at 10.5% moisture on a 15° slope. Goss and Miller [1973] report 2 to 3 kg/t backing fire particulate emissions for burning tower experiments conducted at 7% moisture content in Darley's apparatus, and 3 kg/t for field trials at 7% moisture content. Darley himself, in the 1979 report, attributes the difference between the 1979 data and the 1977 data to the fact that in the later tests, the particulate sampling line

was heated to 150°C. This conclusion is not supported by data on other fuels. Particulate data reported in the 1977 report for barley straw is quite consistent with the data reported in the 1979 report for the same material. Therefore, the particulate emission factor for rice straw in Darley [1979] can only be considered to be of questionable validity. The particle size distributions from the current experiments appear to be in very good agreement with the field data of Goss and Miller [1973].

The discrepancy in SO_2 data between Darley [1979] and the current tests can be attributed directly to the method used by Darley to estimate SO_2 concentrations. Darley computed SO_2 concentrations by means of a mass balance using the sulfur deficit between the ash and the fuel. From an inspection of the current data, this technique overestimates the SO_2 emission, and was thought to do so even by Darley. The question of the fate of the residual sulfur remains even in the current experiments, as it has not been fully accounted. There are three principal possible causes for the discrepancy. The sulfur concentrations measured in the fuel and the ash may be in error, or the direct measurement of SO_2 may be in error, or gas phase sulfur emission is occurring in some other form. The first possibility represents a gross error if the deficit is to be reduced to the levels of SO_2 actually determined. The second cause may be contributing, but a rather large calibration adjustment would be required if the full deficit is to be accommodated. The third possibility was also suggested by Darley [1979], as analyses of combustion products in his experiments had shown that other sulfur containing compounds were present, but unidentified. A combination of all three reasons is likely. It appears that this question requires additional investigation.

The higher NO_x emissions of Darley could be due to differences in the residence times at elevated temperature in the combustion zones of the two simulators. Sufficient data does not exist to determine if the differences are significant, however. Both Mast [1986] and Darley [1979] have indicated that gas temperatures in the stack of Darley's burning tower are higher than in the field at the same elevation. Thus some additional NO_x might be formed if the residence time were longer at high temperature. Comparison of the temperature data in the current study taken from the field and from the tunnel show similar durations at elevated temperature. No such data was found for the burning tower trials of Darley. Goss and Miller [1973] have published time-temperature relationships for heading and backing fires in the field, although the specific manner in which the data were obtained is not reported. Their data suggest that the temperature of a thermocouple suspended above the fuel bed would remain above 100°C for 2 to 2.5 minutes, whereas the duration for a heading fire would be 50 to 60 s. The data for the backing fire have not been reproduced here when conducting field burning experiments in spread straw. The data presented by Goss and Miller may be interpreted to reflect the superposition of three burning fronts, each with a duration approximating that of the heading fire. In field experiments here, the only method producing a temperature history similar to that of the backing fire described by Goss and Miller was burning windrows of straw cut at ground level, such that the loading rate was high, and the fuel layer was deep, a burning practice no longer followed. For the current practice of burning spread fuel, the duration at elevated temperature appears to be similar for heading and backing fires. The spreading velocity of the heading fire is larger than that of the backing fire, and suggests that the burning length is

longer for a heading fire than for a backing fire, which would help to explain the greater smoldering behind the flame in the heading fire. It appears at any rate that the residence times in the wind tunnel backing fires are comparable to those in the field with similar fuel conditions. Further investigation is needed to adequately assess the similarity of the tunnel conditions to the field, however.

References

Albini, F.A. 1976. Estimating wildfire behavior and effects. USDA Forest Service General Technical Report INT-30, Intermountain Forest and Range Experiment Station, Ogden, UT.

Altenkirch, R.A., R. Eichhorn and P.C. Shang. 1980. Buoyancy effects on flames spreading down thermally thin fuels. Combustion and Flame 37:71-83.

Anderson, H.E. and R.C. Rothermel. 1965. Influence of moisture and wind upon the characteristics of free-burning fires. Tenth International Symposium on Combustion, 1009-1019.

Baker, C.J. and R.G. Gawthorpe. 1983. The effect of turbulence simulations on the wind induced loads on ground vehicles. Aerodynamics of Transportation II. American Society of Mechanical Engineers, New York.

Berlad, A.L., R.C. Rothermel and W. Frandsen. 1971. The structure of some quasi-steady fire spread waves. Thirteenth International Symposium on Combustion, 927-933.

Boubel, R.W., E.F. Darley and E.A. Schuck. 1969. Emissions from burning grass stubble and straw. APCA Journal, 19(7):497-500.

CARB. 1988. A procedure relating to the determination of agricultural/forestry waste emission offset credits. California Air Resources Board, Sacramento, CA.

Carrier, G.F., R.E. Fendell, R.D. Fleeter, N. Gat and L.M. Cohen. 1984. Laboratory modelling of aspects of large fires. DNA-TR-84-18, Defense Nuclear Agency, Washington, D.C.

Carroll, J.J. 1973. Determination of temperature, winds and particulate concentrations in connection with open field burning. Final report, ARB Project 2114, Department of Agricultural Engineering, University of California, Davis, CA.

Carroll, J.J., Miller, G.E., Thompson, J.F. and E.F. Darley. 1977. The dependence of open field burning emissions and plume concentrations on meteorology, field conditions, and ignition techniques. Atmos. Environ. 11:1037-1050.

Cermak, J.E. 1971. Laboratory simulation of the atmospheric boundary layer. AIAA Journal 9(9):1746-1754.

Cermak, J.E. 1975. Simulation of atmospheric boundary layers in wind tunnels. Atmospheric Technology 7:66-71.

Chandler, C., P. Cheney, P. Thomas, L. Trabaud and D. Williams. 1983. Fire in forestry, Vol. 1: Forest fire behavior and effects. John Wiley and Sons, New York, NY.

Cionco, R.M. 1972. Intensity of turbulence within canopies with simple and complex roughness elements. Boundary-layer Meteorology 2:453-465.

Curry, J.R. and W.L. Fons. 1938. Rate of spread of surface fires in the ponderosa pine type of California. Journal of Agricultural Research 57(4):239-267.

Darley, E. F. 1979. Hydrocarbon characterization of agricultural waste burning. Final Report, CAL/ARB Project A7-068-30, Statewide Air Pollution Research Center, University of California, Riverside, CA.

Darley, E.F. 1972. Air pollution from forest and agricultural burning. CARB Project 2-017-1, University of California, Riverside, CA.

Darley, E.F. 1977. Emission factors from burning agricultural wastes collected in California. Final Report, CA/ARB Project 4-011, Statewide Air Pollution Research Center, University of California, Riverside, CA.

Darley, E.F., F.R, Burleson, E.H. Mateer, J.T. Middleton and V.P. Osterli. 1977. Contribution of burning of agricultural wastes to photochemical air pollution. APCA Journal, 16(12):685-690.

de Ris, J.N. 1969. Spread of a laminar diffusion flame. Twelfth International Symposium on Combustion, 241-252.

Emmons, H. 1964. Fire in the forest. Fire Research Abstracts and Reviews 5(3):163-178.

Emmons, H.W. and T. Shen. 1971. Fire spread in paper arrays. Thirteenth International Symposium on Combustion, 917-926.

EPA. 1973. Compilation of air pollutant emission factors. U.S. Environmental Protection Agency, Office of Air Programs publication AP-42.

Finnigan, J.J. and P.J. Mulhearn. 1978. Modelling waving crops in a wind tunnel. Boundary-layer Meteorology 14:253-277.

Fleeter, R.D., F.E. Fendell, L.M. Cohen, N. Gat and A.B. Witte. 1984. Laboratory facility for wind aided firespread along a fuel matrix. Combustion and Flame 57:289-311.

Fons, W.L. 1946. Analysis of fire spread in light forest fuels. Journal of Agricultural Research 72(13): 93-121.

Frandsen, W.H. 1971. Fire spread through porous fuels from the conservation of energy. Combustion and Flame 16:9-16.

Frey, A.E. and J.S. T'ien. 1979. A theory of flame spread over a solid fuel including finite-rate chemical kinetics. Combustion and Flame 36:263-289.

Goss, J.R. and G.E. Miller. 1973. Study of abatement methods and meteorological conditions for optimum dispersion of particulates from field burning of rice

straw. Unpublished report, ARB Project 1-101-1, University of California, Davis, CA.

Hottel, H.C., G.C. Williams and F.R. Steward. 1965. The modeling of firespread through a fuel bed. Tenth International Symposium on Combustion, 997-1007.

Kosdon, F.J., F.A. Williams and C. Buman. 1969. Combustion of vertical cellulosic cylinders in air. Twelfth International Symposium on Combustion, 253-264.

Lastrina, F.A., R.S. Magee and R.F. McAlevy III. 1971. Flame spread over fuel beds: solid-phase energy considerations. Thirteenth International Symposium on Combustion, 935-948.

Lumley, J.L. and H.A. Panofsky. 1964. The structure of atmospheric turbulence. John Wiley and Sons, New York.

McAlevy, R.F. and R.S. Magee. 1969. The mechanism of lame spreading over the surface of igniting condensed-phase materials. Twelfth International Symposium on Combustion, 215-227.

McBean, G.A. 1971. The variations of the statistics of wind, temperature and humidity fluctuations with stability. Boundary-layer Meteorology 1:438-457.

Maitani, T. 1979. A comparison of turbulence statistics in the surface layer over plant canopies with those over several other surfaces. Boundary-layer Meteorology 17:213-222.

Mast, T.J. 1986. Mutagenicity and chemical characterization of organic constituents on rice straw smoke particulate matter. Unpublished Ph.D. thesis, University of California, Davis, CA.

Mobley, H.E., editor. 1976. Southern forestry smoke management guidebook. USDA Forest Service, Southeastern Forest Experiment Station, Asheville, NC, and Southern Forest Fire Laboratory, Macon, GA.

Nieuwstadt, F.T.M. and H. van Dop. 1982. Atmospheric turbulence and air pollution modelling. D. Reidel Publishing Co., Dordrecht, Holland.

Ohtou, A., T. Maitani and T. Seo. 1983. Direct measurement of vorticity and its transport in the surface layer over a paddy field. Boundary-layer Meteorology 27:197-207.

Oregon Department of Environmental Quality. 1979. Open field burning: an emission factors study of alternative firing techniques. Portland, OR.

Ohtaki, E. 1980. Turbulent transport of carbon dioxide over a paddy field. Boundary-layer Meteorology 19:315-336.

Panofsky, H.A. and J.A. Dutton. 1984. Atmospheric turbulence. John Wiley and Sons, New York.

Pasquill, F. 1974. Atmospheric diffusion. John Wiley and Sons, New York.

Plate, E. 1982. Engineering meteorology. Elsevier Scientific, Amsterdam.

Raabe, O.G. 1968. A general method for fitting size distributions to multicomponent aerosol data using weighted least-squares. Environmental Science and Technology 12(10):1162-1167.

Rothermel, R.C. 1967. Airflow characteristics--wind tunnels and combustion facilities, Northern Forest Fire Laboratory. USDA Forest Service, Intermountain Forest and Range Experiment Station, Missoula, MT.

Rothermel, R.C. 1972. A mathematical model for predicting fire spread in wildland fuels. USDA Forest Service, Intermountain Forest and Range Experiment Station, Ogden, UT.

Rothermel, R.C. 1983. How to predict the spread and intensity of forest and range fires. USDA Forest Service, Intermountain Forest and Range Experiment Station, Ogden, UT.

Rothermel, R.C. and H.E. Anderson. 1966. Fire spread characteristics determined in the laboratory. USDA Forest Service, Intermountain Forest and Range Experiment Station, Ogden, UT.

Seginer, I., P.J. Mulhearn, E.F. Bradley and J.J. Finnigan. 1976. Turbulent flow in a model plant canopy. Boundary-layer Meteorology 10:423-453.

Sneeuwjagt, R.J. and W.H. Frandsen. 1977. Behavior of experimental grass fires vs. predictions based on Rothermel's fire model. Canadian Journal of Forest Research 7(2):357-367.

Sutton, O.G. 1960. Atmospheric turbulence. John Wiley and Sons, New York, NY.

Wichman, I.S. 1983. Flame spread in an opposed flow with a linear velocity gradient. Combustion and Flame 50:287-304.

Wichman, I.S., F.A. Williams and I. Glassman. 1982. Theoretical aspects of flame spread in an opposed flow over flat surfaces of solid fuels. Nineteenth International Symposium on Combustion, 835-845.

Williams, F.A. 1982. Urban and wildland fire phenomenology. Progress in Energy and Combustion Science 8:317-354.

Williams, F.A. 1985. Combustion Theory. Benjamin/Cummings Publishing Co., Menlo Park, California.

Williams, F.A. 1989. Evaluation of the test facility at UC Davis for determining emissions from open burning of agricultural and forestry wastes. Report to the California Air Resources Board, Sacramento, CA.

Nomenclature

Symbol	Description	Units
A_i	constant depending on direction i	---
B	preexponential factor for gas phase reaction	m^3/mol-s
B_{ij}	quantity of biomass of type j used during month i	t
c_p	thermal capacity of gas	kJ/kg-K
c_s	thermal capacity of solid	kJ/kg-K
D	Damkohler number	---
d_o	zero plane displacement	m
E	activation energy for gas phase reaction	kJ/mol
EF_j	emission factor of pollutant from biomass of type j	kg/t
g	gravitational acceleration	m/s^2
HBF_j	fraction of total biomass j that is openly burned	---
I_1	turbulence intensity in the streamwise direction	---
k	von Karman's constant (=0.4)	---
K_m	eddy diffusivity	m^2/s
L	Monin-Obukhov length scale	m
m_{ox}	oxygen mass fraction in ambient fluid	---
P	pollutant offset credit	kg/day
Q	negative of the enthalpy of reaction	kJ/kg
R	universal gas constant	kJ/mol-K
t	half thickness of fuel element	m
T_∞	temperature of ambient fluid	K
T_f	flame temperature	K
T_v	vaporization temperature for solid pyrolysis	K
u	mean velocity of the wind in the streamwise direction	m/s
u'	velocity fluctuation from the mean wind in the streamwise direction	m/s

$u*$	friction velocity	m/s
V_F	fire propagation velocity	m/s
V	dimensionless fire propagation velocity	---
w	vertical velocity component	m/s
W_{ox}	molecular weight of oxygen	kg/kg-mol
x	emission offset fraction depending on origin of biomass delivered to a conversion facility	---
z	elevation normal to the surface	m
z_o	surface roughness parameter	m
σ_i	standard deviation of velocity in i direction	m/s
λ	gas thermal conductivity	kW/m-K
μ	fluid viscosity	kg/m-s
ν	kinematic viscosity	m^2/s
ρ	gas density	kg/m^3
ρ_s	solid density	kg/m^3
τ	Reynolds stress component	Pa

Table 1. Fuel and ash analysis for combustion trials of 1 September and 7 September, 1988, in rice straw.

	1 September		7 September	
	Fuel	Ash	Fuel	Ash
Proximate Analysis:				
Moisture (% wet basis)	6.5	2.8	7.3	3.3
Ash (% dry basis)	13.59	78.41	13.16	77.68
Volatiles (% dry basis)	69.44	11.11	69.94	10.34
Fixed Carbon (% dry basis)	16.97	10.48	16.90	11.98
Higher Heating Value (MJ/kg, dry basis)	15.91	4.99	15.99	5.34
Ultimate Analysis (% dry basis):				
Carbon	40.41	11.17	40.29	15.23
Hydrogen	5.42	0.49	5.39	0.56
Oxygen (by difference)	38.69	4.05	38.98	3.18
Nitrogen	0.53	0.24	0.69	0.31
Sulfur	0.05	0.09	0.08	<0.02
Chlorine	0.20	0.06	0.27	<0.02
Residual	14.7	83.9	14.3	80.7

Table 2. Material balances and fire characteristics for tests of 1 September and 7 September in rice straw.

	1 September	7 September
Fire Characteristics:		
Effective fuel loading (g/m^2 wet basis)	584	577
Fuel consumption (g wet basis)	23,190	22,896
Fuel moisture (% wet basis)	6.5	7.3
Dry Fuel consumption (g)	21,683	21,225
Burn duration (minutes)	34	35
Dry fuel consumption rate (g/s)	10.63	10.11
Fire Propagation Velocity (m/min)	0.96	0.93
Mean wind velocity (m/s)	2.35	2.35
Mean air temperature (°C)	37	32
Mean relative humidity (%)	15	15
Air density (kg/m^3)	1.140	1.159
Air flowrate (g/s)	3,982	4,048
Overall air/fuel ratio (dry basis)	375	400
Stack gas mass flowrate (g/s)	3,991	4,057
Stack gas temperature (°C)	53	48
Stack gas flowrate at temperature (m^3/s)	3.68	3.68
Ash Recovery:		
Total ash recovered (g)	3,993	3,538
Moisture content (% wet basis)	2.8	3.3
Dry ash recovery (g)	3,881	3,421
Fraction of dry fuel consumption (%)	17.9	16.1
Inorganic fraction of fuel (%)	14.7	14.3
Inorganic fraction of ash (%)	83.9	80.7
Expected ash recovery (% of fuel)	17.5	17.7

Table 2 (continued). Material balances and fire characteristics for tests of 1 September and 7 September in rice straw.

	1 September	7 September
Nitrogen:		
Fuel nitrogen (% dry basis)	0.53	0.69
Ash nitrogen (% dry basis)	0.24	0.31
NO concentration in stack (ppm)	3.0	2.8
NO_2 concentration in stack (ppm)	0.9	0.6
Fuel N (g)	115	146
Ash N (g)	9	11
Gas phase N from NO, NO_2 (g)	15	14
Excess Fuel N (g)	91	121
Sulfur:		
Fuel sulfur (% dry basis)	0.05	0.08
Ash sulfur (% dry basis)	.09	<0.02
SO_2 concentration in stack (ppm)	0.12	0.25
Fuel S (g)	11	17
Ash S (g)	3	<1
Gas phase S from SO_2 (g)	1	2
Excess Fuel S (g)	7	14
Carbon:		
Fuel carbon (% dry basis)	40.41	40.29
Ash carbon (% dry basis)	11.17	15.23
Stack gas concentrations (ppm, excludes background):		
CO_2	2,000	2,000
CO	168	155
CH_4	8	4
C_2H_2	0.3	0.2
C_2H_4	1.7	1.7
C_2H_6	0.2	0.13
C_6H_6	0.137	0.082
Fuel C (g)	8,762	8,552
Ash C (g)	436	521
Gas phase C (g)	7,346	7,617
Particulate C (g)	ND	ND
Excess Fuel C (g)	980	414
Closure (%)	89	95

Table 3. Particulate concentrations and size distributions for combustion trials of 1 September and 7 September, 1988, in rice straw.

		1 September		7 September	
			cumulative		cumulative
		mass (mg)	fraction (%)	mass (mg)	fraction (%)
Sierra Impactor:					
Stage	Effective Diameter (μm)				
1	10.400	0.05	100.0	0.02	100.0
2	6.020	0.04	99.3	0.03	99.7
3	3.130	0.10	98.7	0.04	99.2
4	1.880	0.11	97.3	0.01	98.6
5	1.130	0.24	95.8	0.12	98.4
6	0.674	0.60	92.5	0.55	96.5
7	filter	6.03	84.1	5.44	87.6
Concentration (mg/m^3)		11.38		9.86	
Aerodynamic diameter (μm)		0.21		0.32	
σ_g		2.82		1.85	
HTHP Impactor:					
1	12.80	0.11	100.0	0.12	100.0
2	7.64	0.18	97.1	0.17	96.7
3	4.31	0.16	92.3	0.17	92.1
4	1.97	0.15	88.1	0.17	87.5
5	1.30	0.15	84.1	0.27	82.9
6	0.75	0.35	80.1	0.43	75.5
7	0.46	1.16	70.9	0.91	63.8
8	filter	1.52	40.2	1.42	38.9
Concentration (mg/m^3)		9.47		9.17	
Aerodynamic diameter (μm)		0.47		0.51	
σ_g		1.63		2.49	

Table 4. Emission factors (kg/t)[1] for preliminary combustion trials of 1 September and 7 September, 1988, in rice straw (7% moisture), with comparison to Darley [1979] at 14.9% average moisture wet basis.

	1 September	7 September	Average	Darley [1979]
Particulate Matter[2]	3.28	3.34	3.31	1.06
NO	1.16	1.16	1.16	1.88
NO_2	0.54	0.38	0.46	0.65
NO_x (as NO_2)	2.32	2.16	2.24	3.53
SO_2	0.10	0.22	0.16	1.00[3]
CH_4	1.66	0.88	1.27	0.82
C_2H_2	0.10	0.07	0.09	0.11
C_2H_4	0.62	0.66	0.64	0.41
C_2H_6	0.08	0.05	0.07	0.11
C_6H_6	0.14	0.09	0.12	0.05
CO	60.89	59.99	60.44	89.62[4]
CO_2	1,139	1,216	1,178	NR[5]

[1] All values dry basis (zero moisture). Multiply by 2.0 to obtain lb/ton.

[2] Based on results of HTHP impactor. Note that Darley [1977] reports 3.47 kg/t particulate matter (dry basis) for a backing fire in 9.3% moisture rice straw on a 25° slope, and 4.64 kg/t at 10.5% moisture and 15° burning slope.

[3] Darley's value for SO_2 computed from the difference of sulfur in the fuel and ash.

[4] Darley [1977]. Corrected for average moisture of 9.9% wet basis. CO for rice straw is not reported by Darley [1979].

[5] Not Reported.

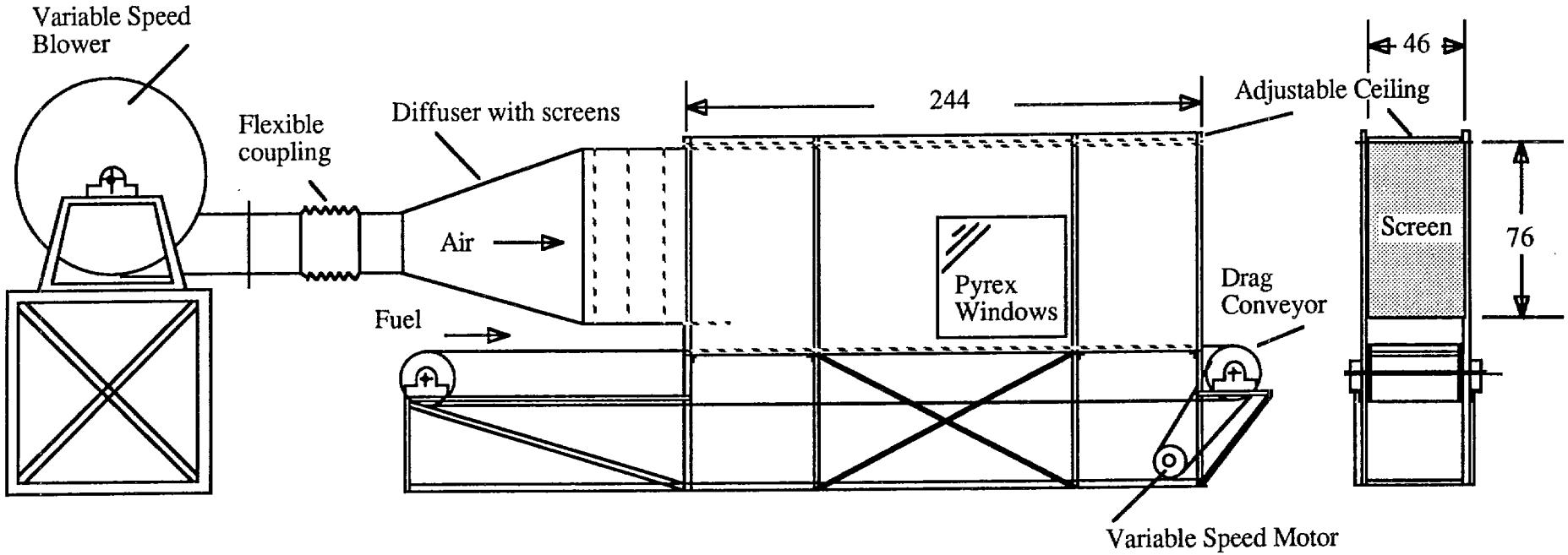

Fig. 1. Schematic of the UCD prototype wind tunnel for maintaining stationary open flames.

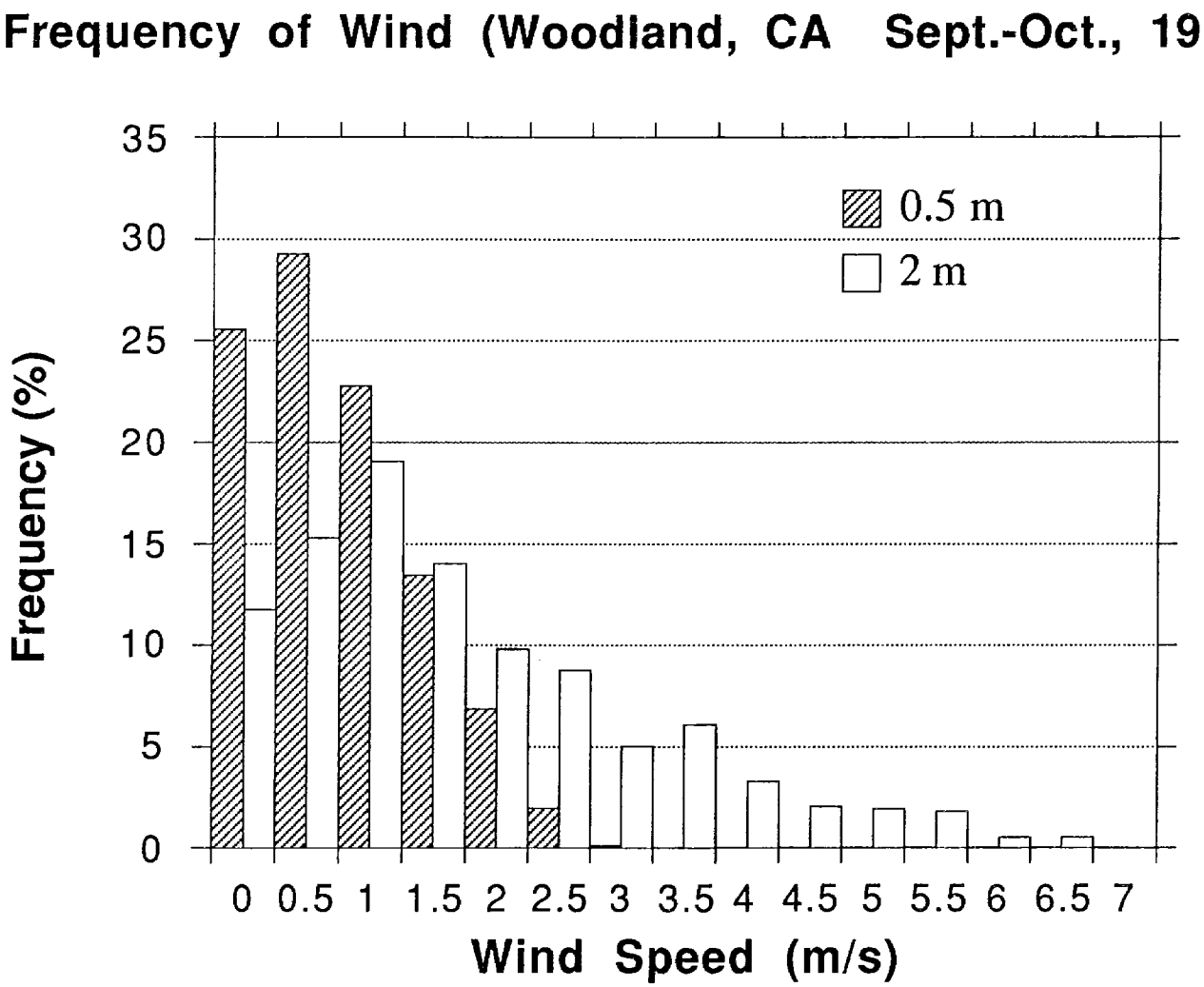

Fig. 2. Frequency of the wind for Woodland, CA during September and October, 1987.

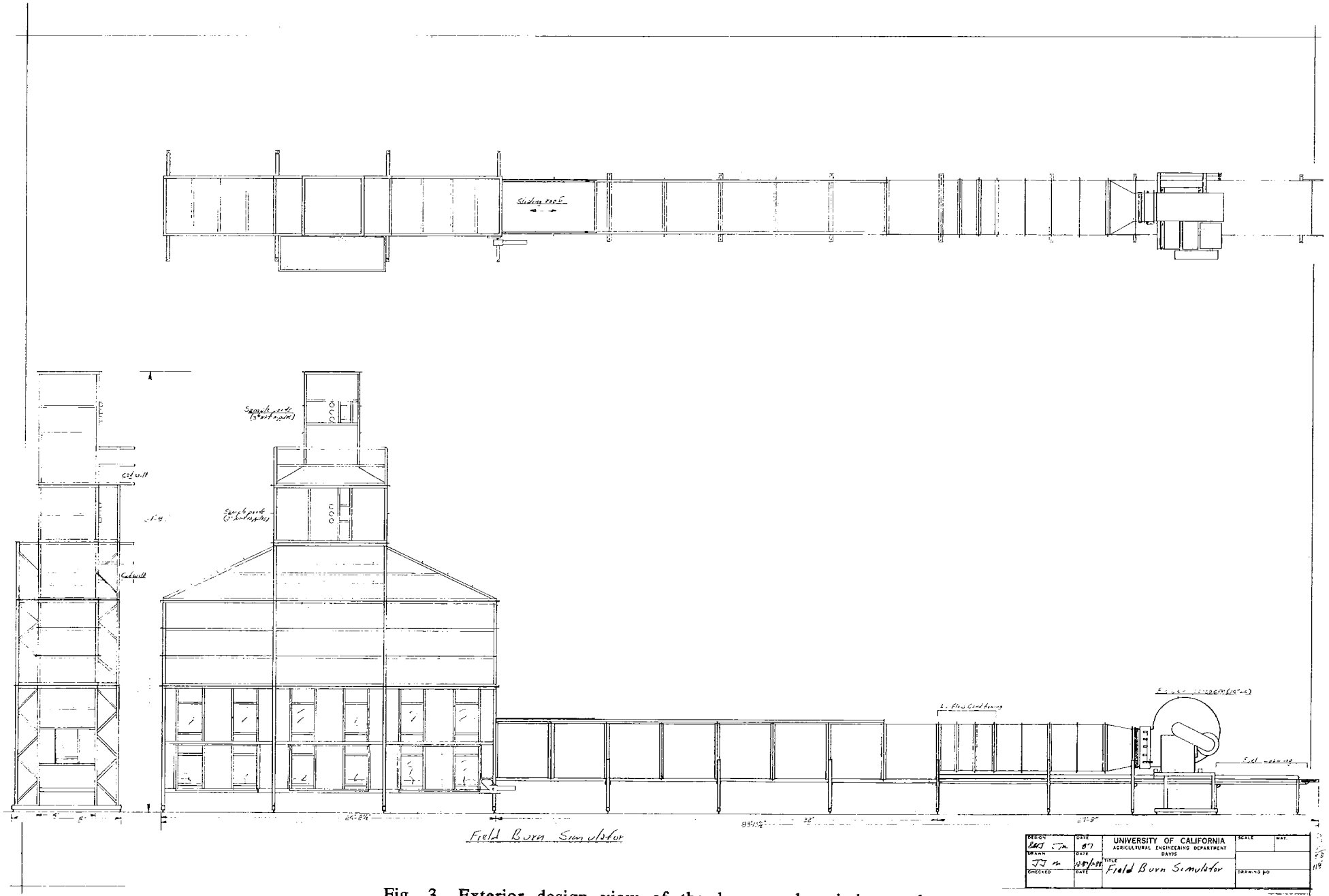

Fig. 3. Exterior design view of the large scale wind tunnel.

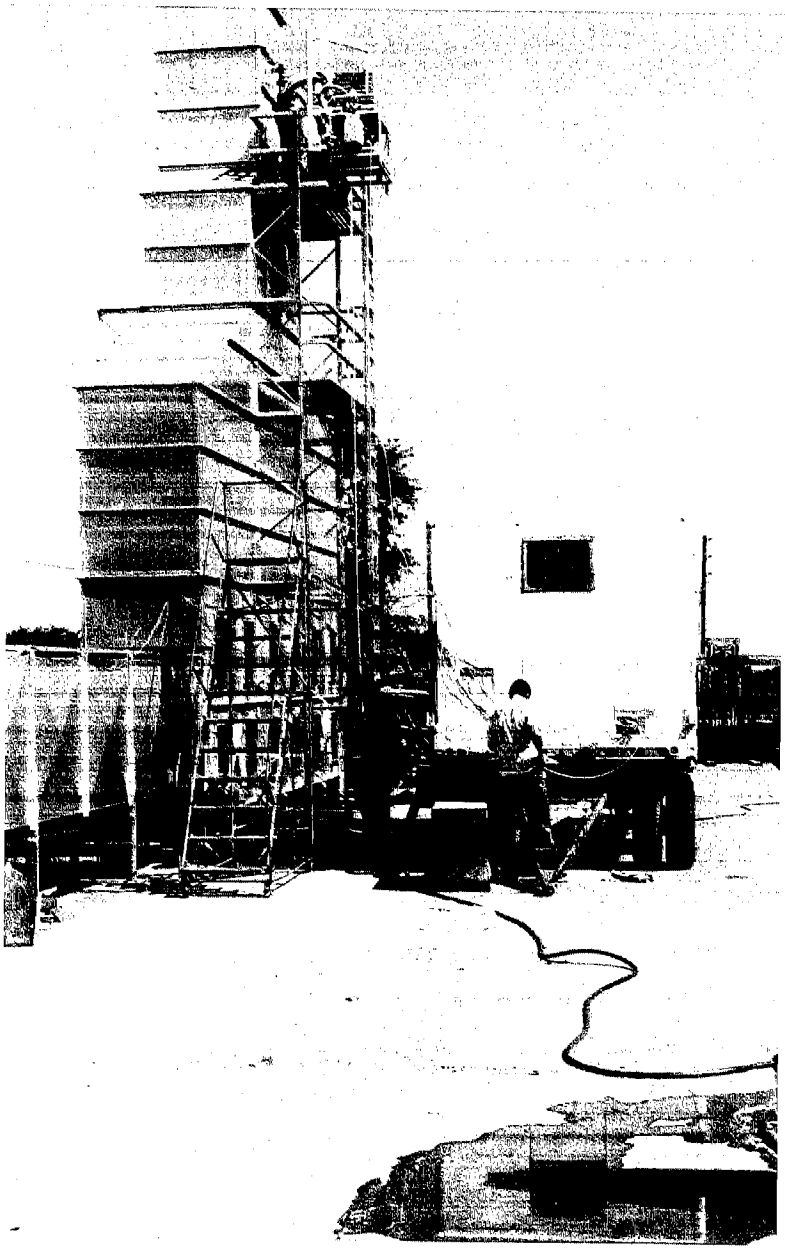

Fig. 4. Photograph of the large scale wind tunnel showing flow development section, combustion test section, sampling stack, and instrument trailer.

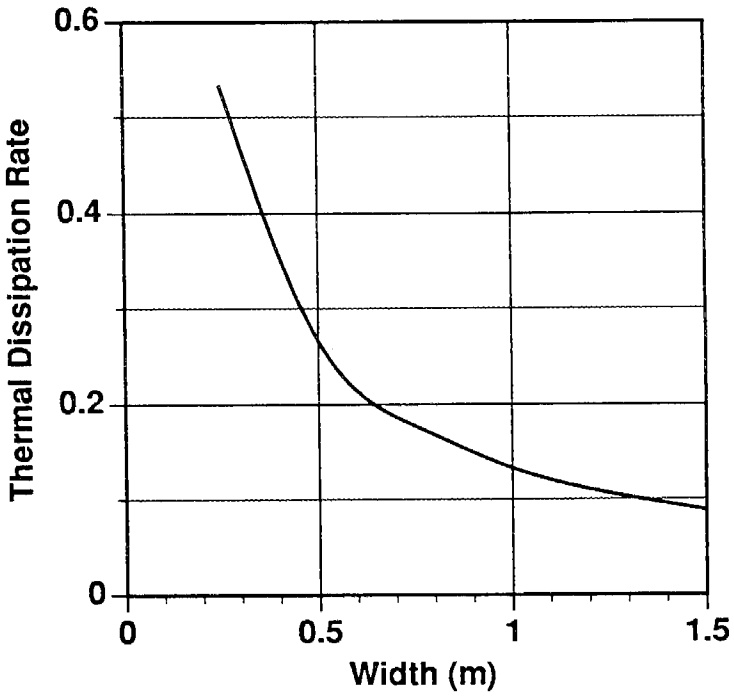

Fig. 5. Wall thermal dissipation rate (dimensionless) as a function of the wind tunnel width.

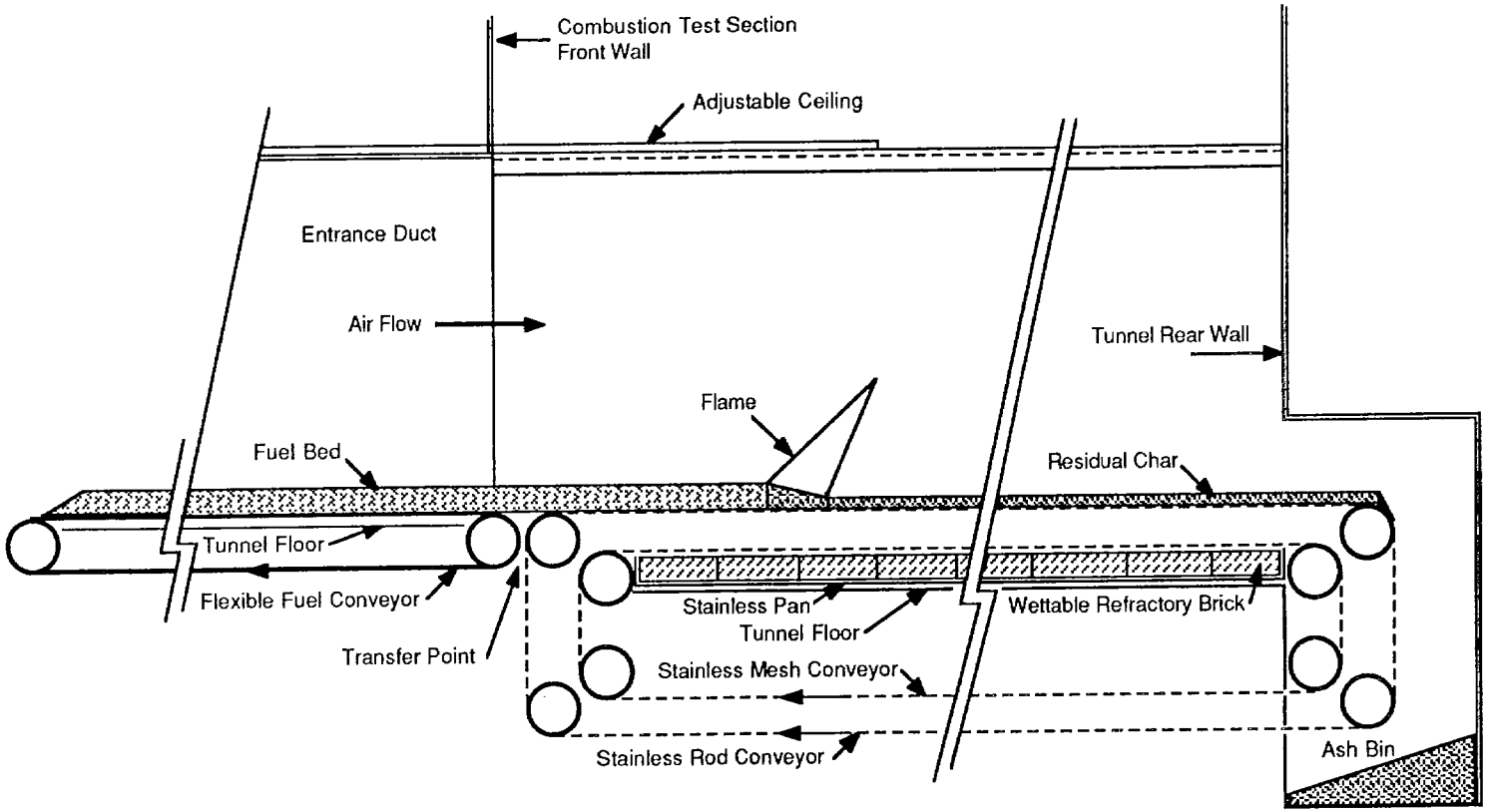

Fig. 6. Schematic of the fuel conveyor system for the large scale wind tunnel.

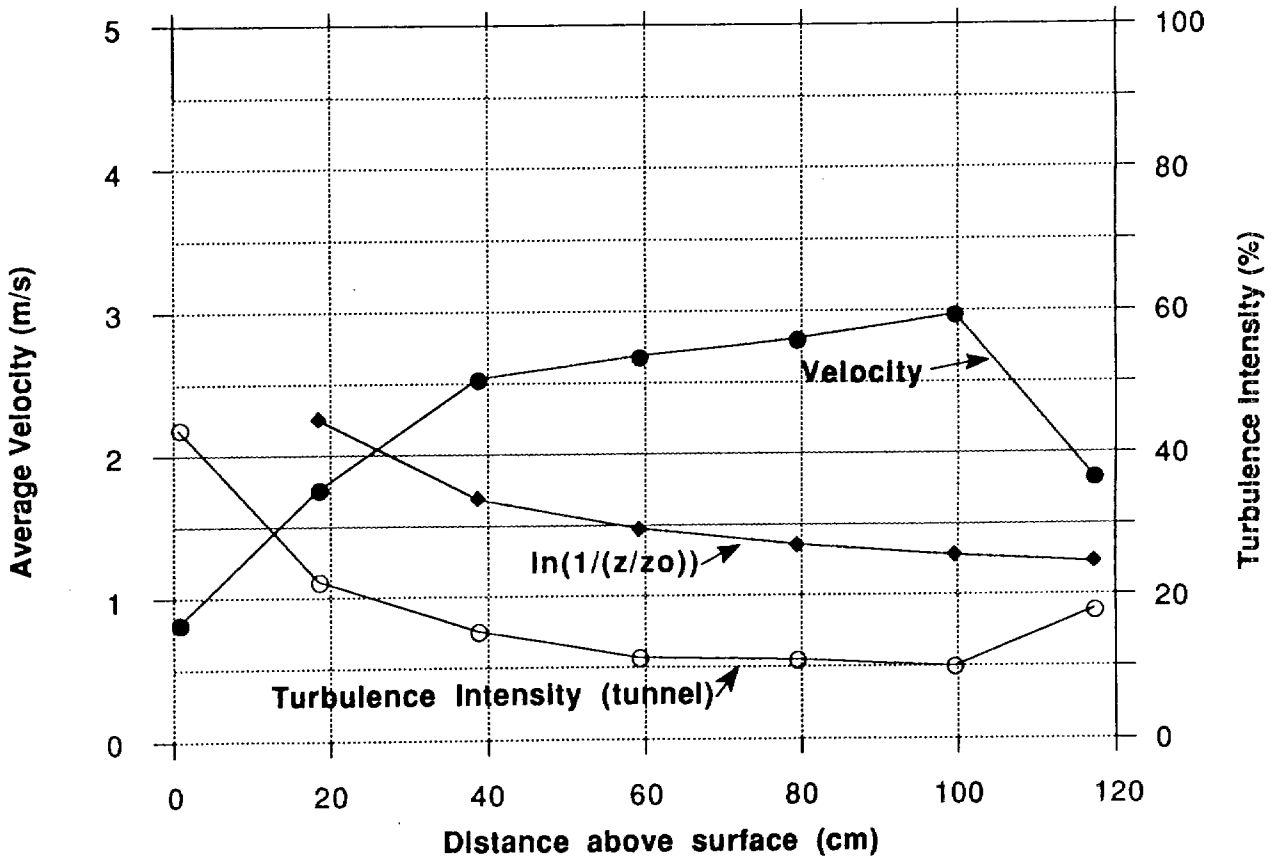

Fig. 7. Vertical velocity profile and turbulence intensity at the entrance to the combustion test section. Shown for comparison is the computed turbulence intensity of the field estimated for a grass surface.

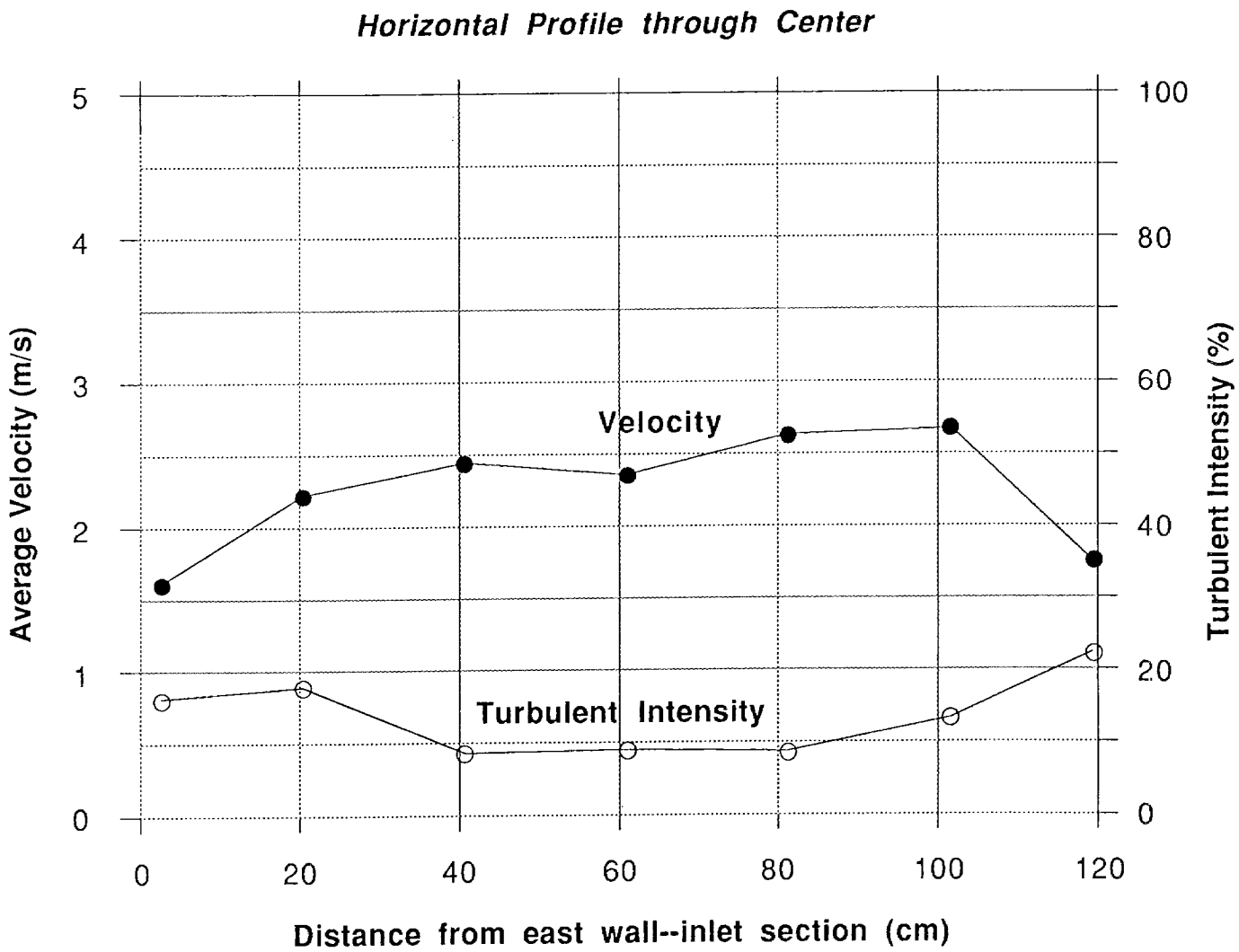

Fig. 8. Horizontal velocity profile and turbulence intensity at the entrance to the combustion test section.

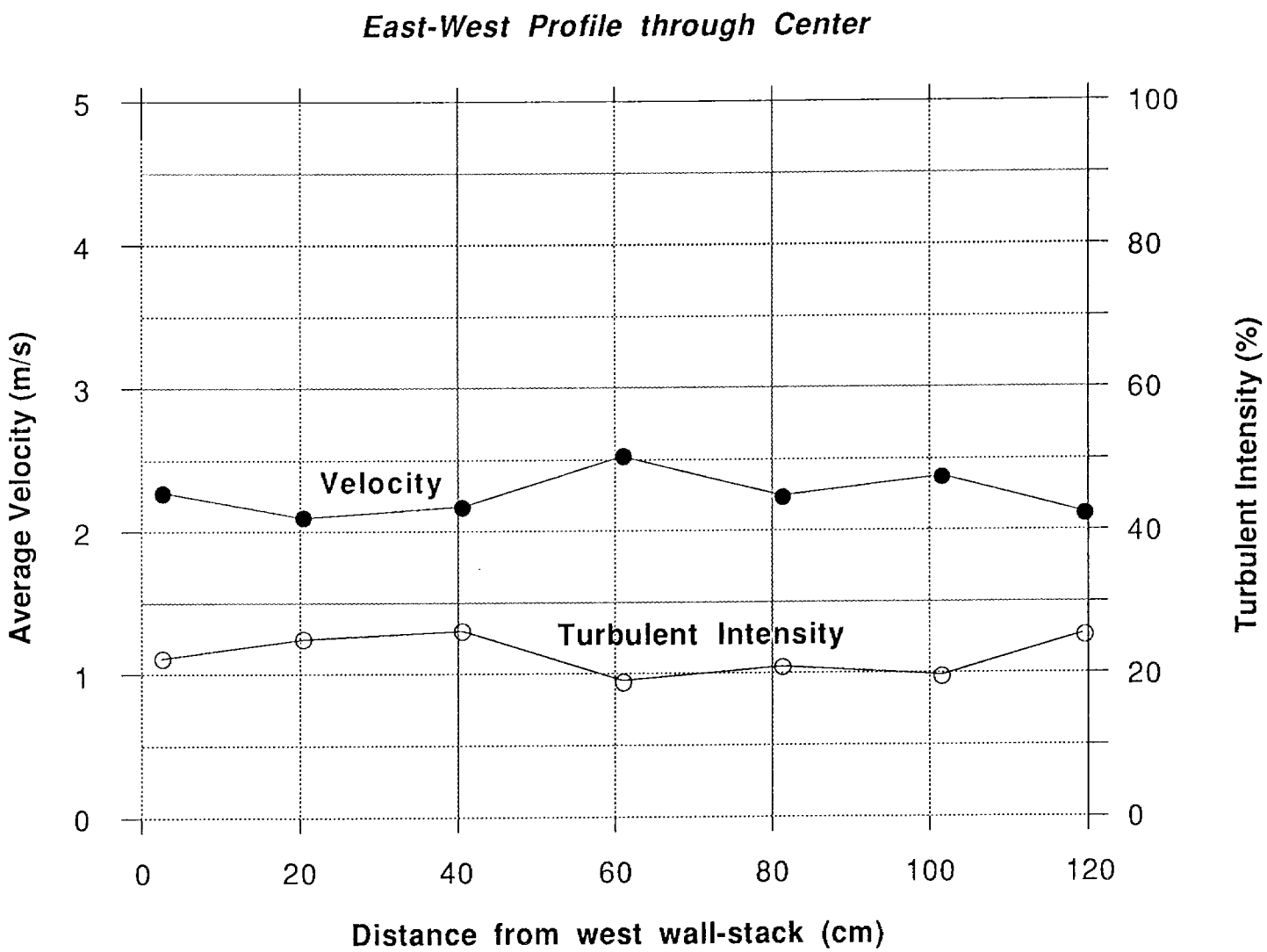

Fig. 9. Lateral velocity profile and turbulence intensity across the sampling stack.

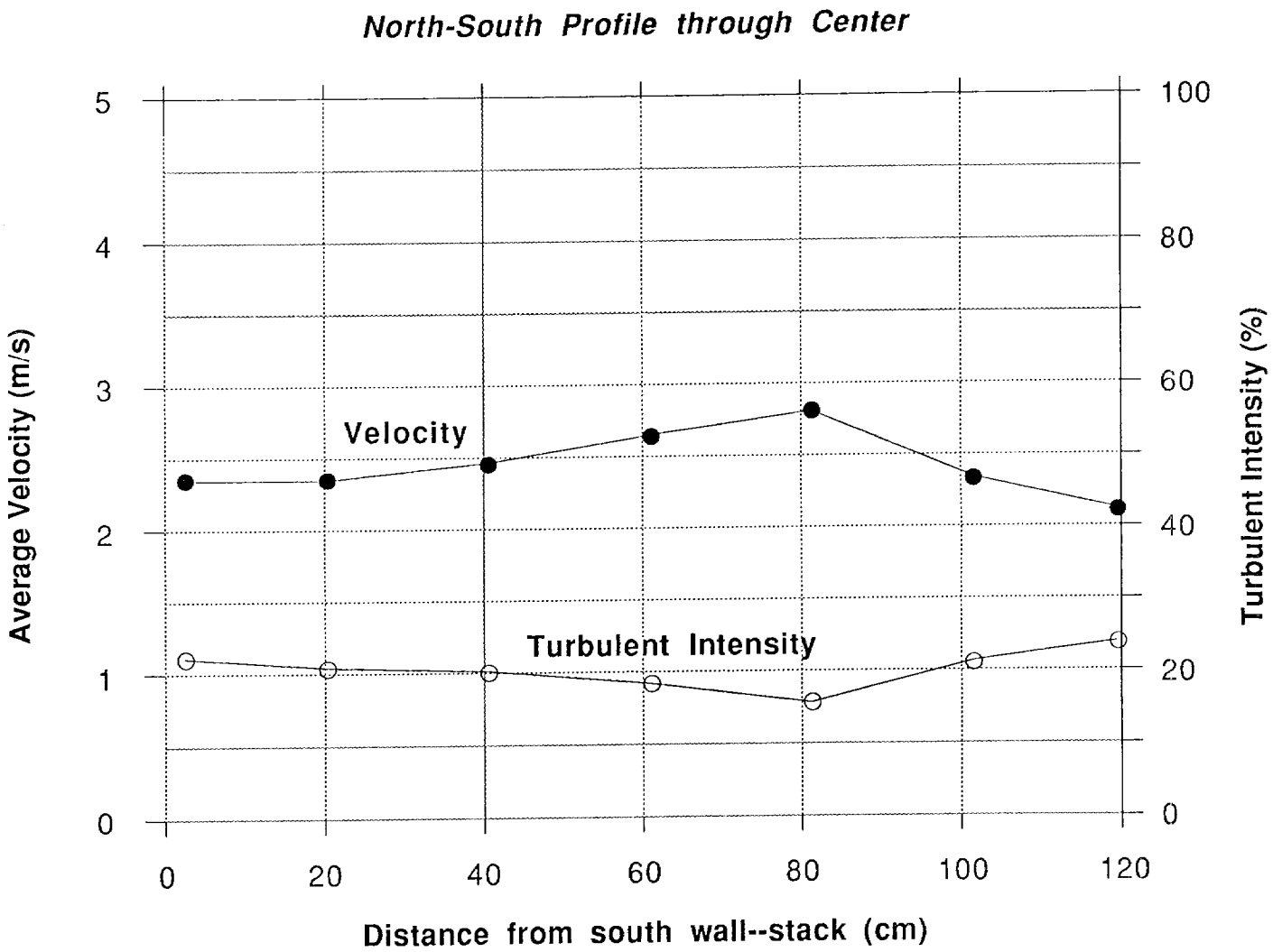

Fig. 10. Longitudinal velocity profile and turbulence intensity across the sampling stack.

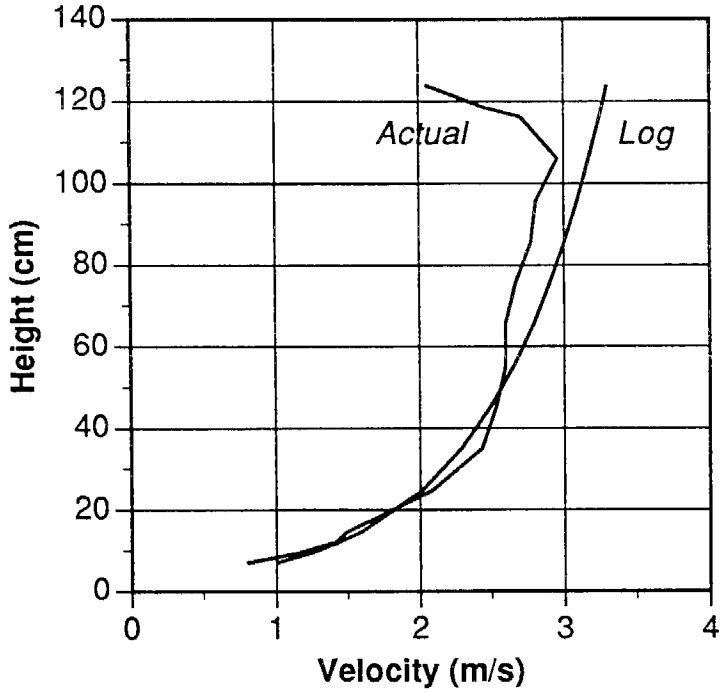

Fig. 11. Comparison of the actual inlet vertical velocity profile to a logarithmic law of the wall profile based on a 5 cm high grass surface ($u* = 0.32$, $z_o = 0.02$, $d_o = 0$).

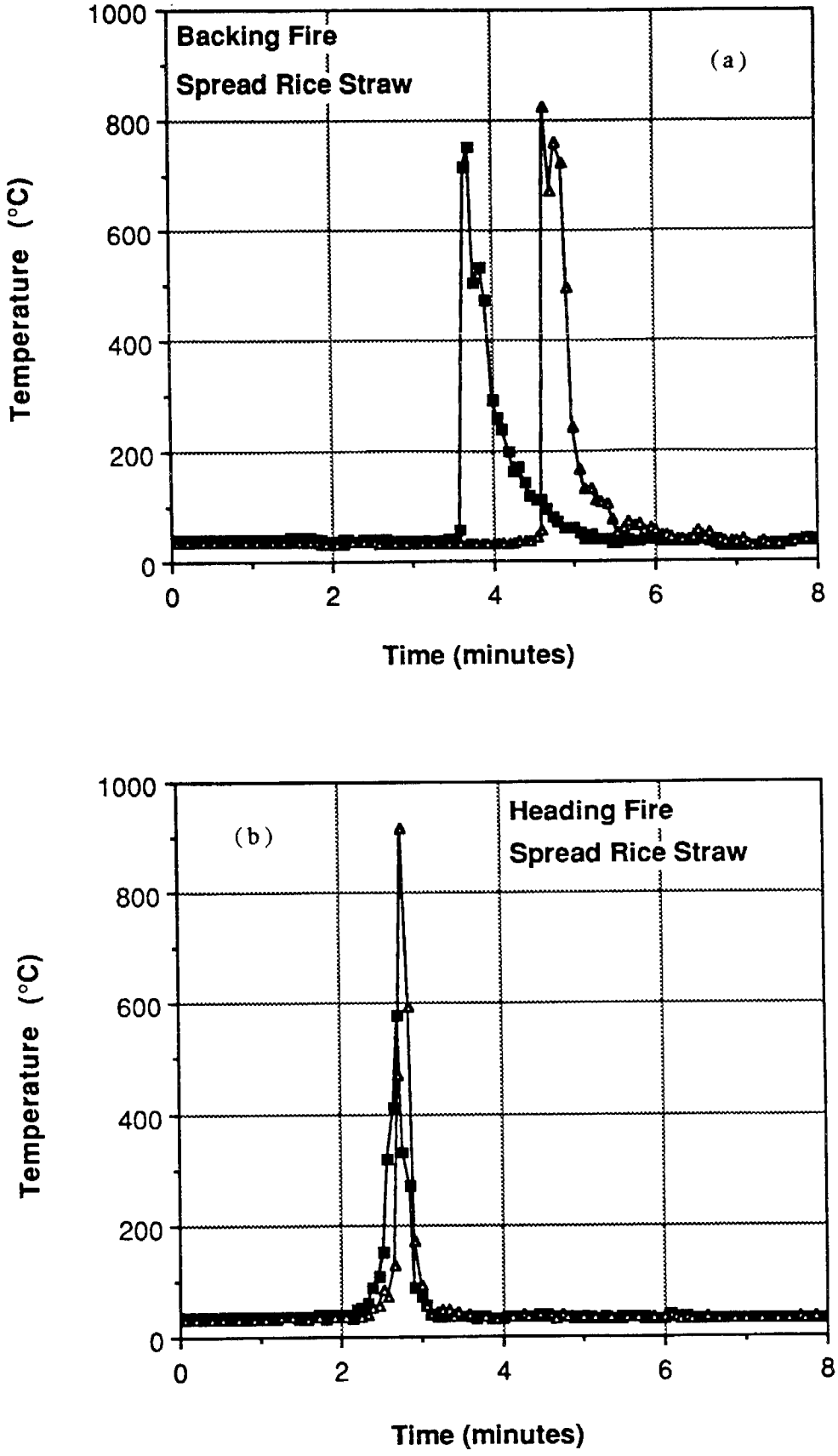

Fig. 12. Temperature at the fuel surface for field burns in rice straw conducted as backing (a) and heading (b) fires. Data from two thermocouples separated horizontally by 0.95 m are shown.

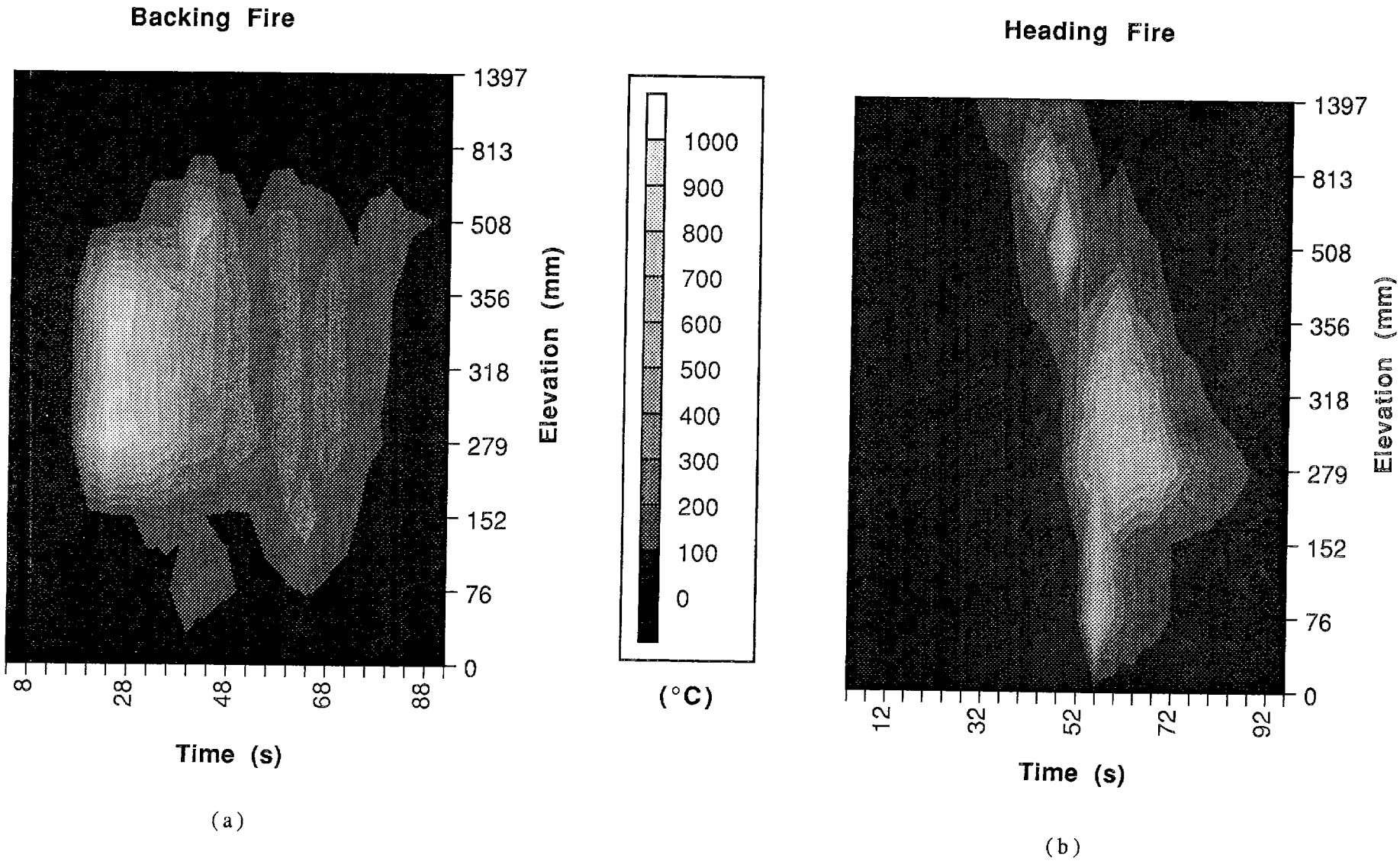

(a)

(b)

Fig. 13. Temperature contour maps generated from a vertical array of thermocouples during field tests of backing (a) and heading (b) fires in rice straw. The vertical (elevation) scale is exaggerated.

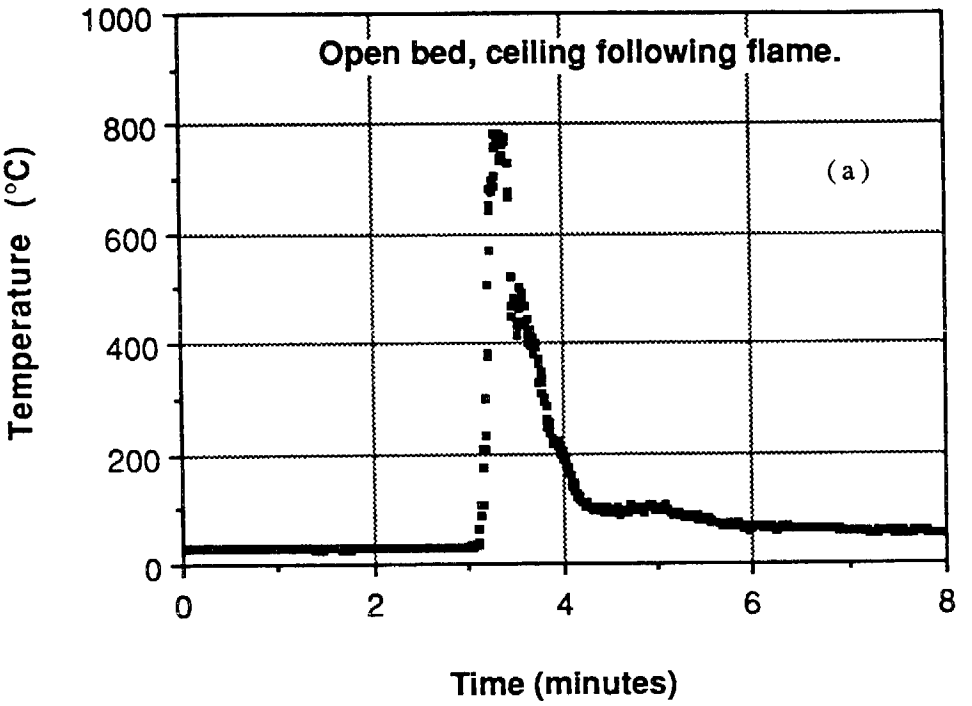

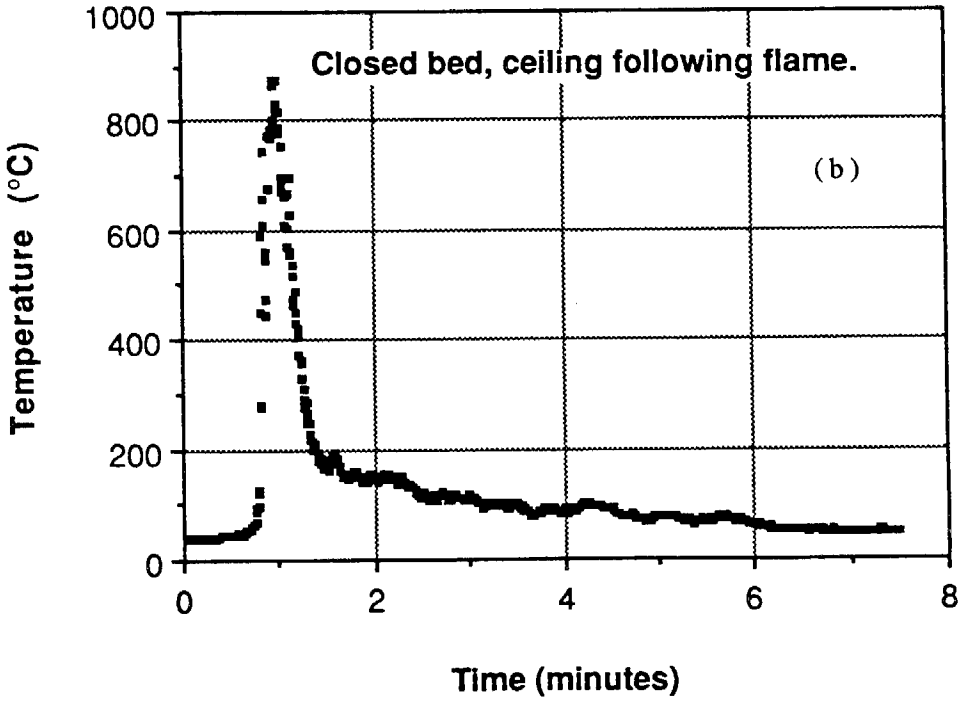

Fig. 14. Wind tunnel temperature histories for fires in rice straw burning past a thermocouple at the fuel surface: (a) fuel carried on the rod conveyor and open below, with the ceiling extended to the leading edge of the fire, (b) ceiling extended but with a steel sheet inserted just below the rod conveyor, (c) ceiling retracted with the fuel bed open from below, and (d) ceiling retracted with a steel sheet inserted below the rod conveyor.

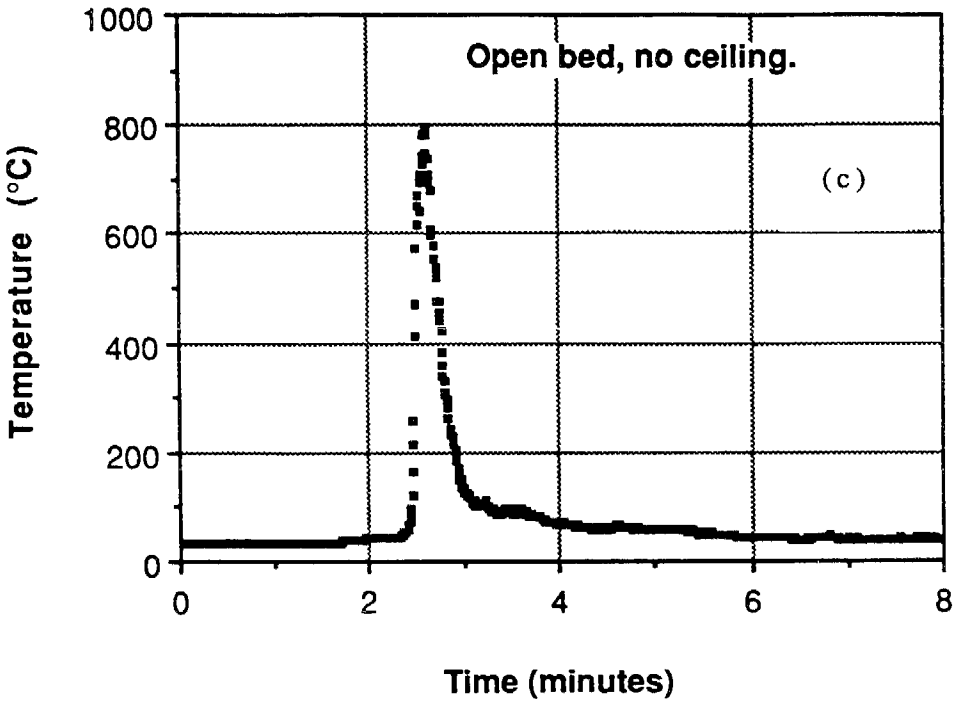

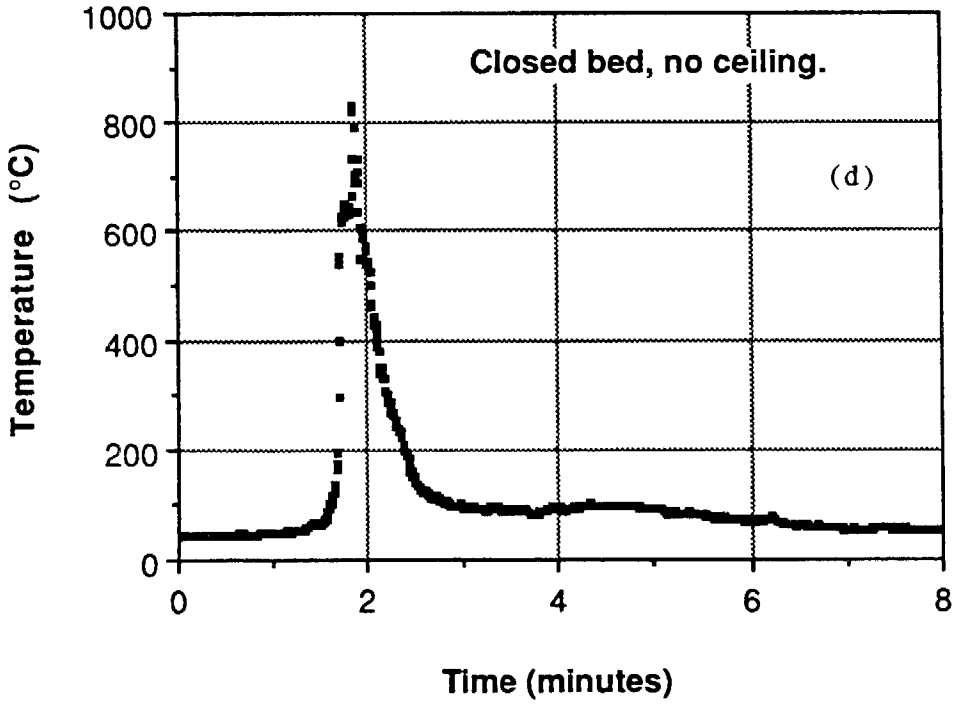

Fig. 14. (continued)

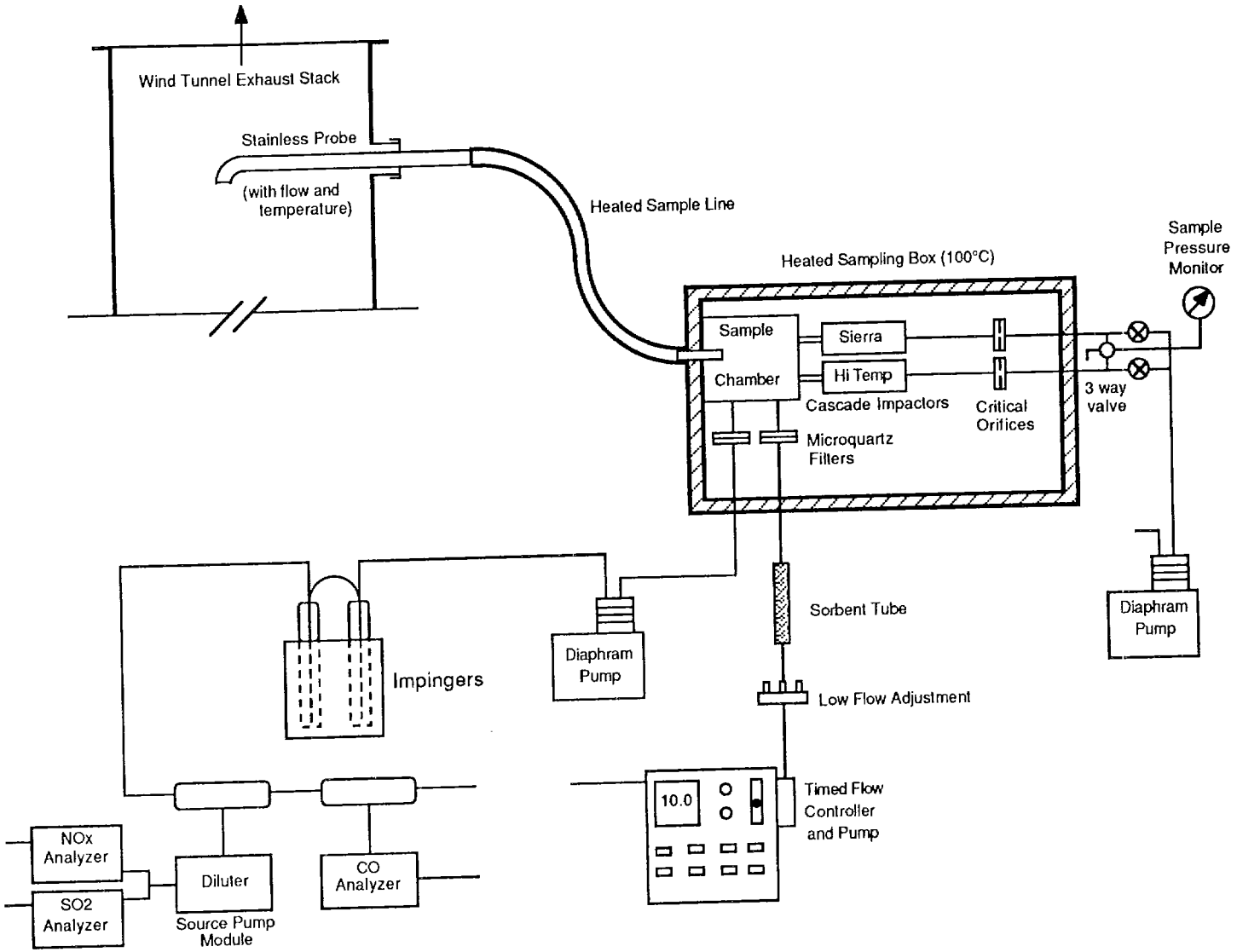

Fig. 15. Sampling train used to collect particulate, volatile organic, and gas samples from the sampling stack of the large scale wind tunnel.

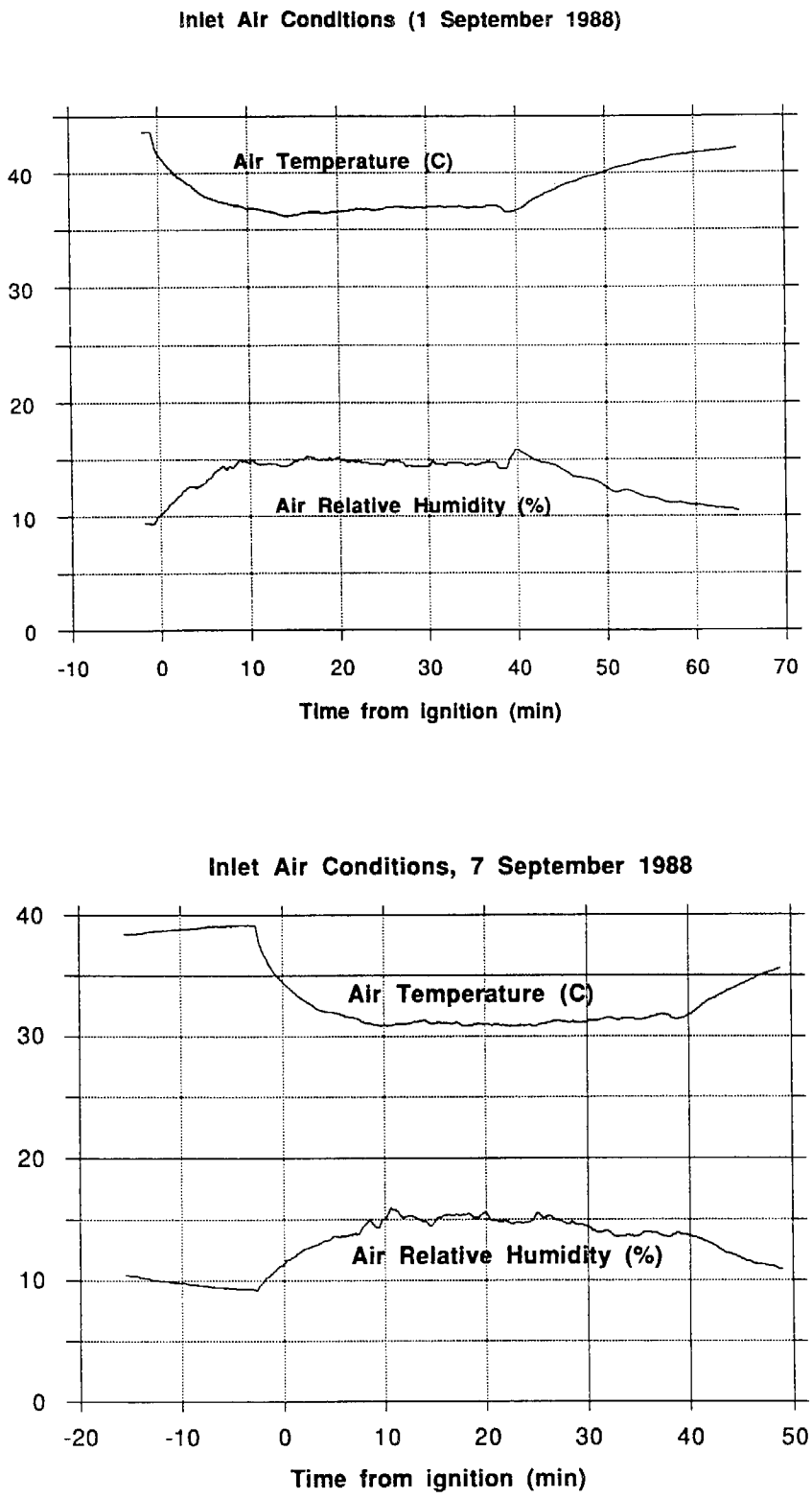

Fig. 16. Inlet air conditions for the tests of 1 and 7 September, 1988.

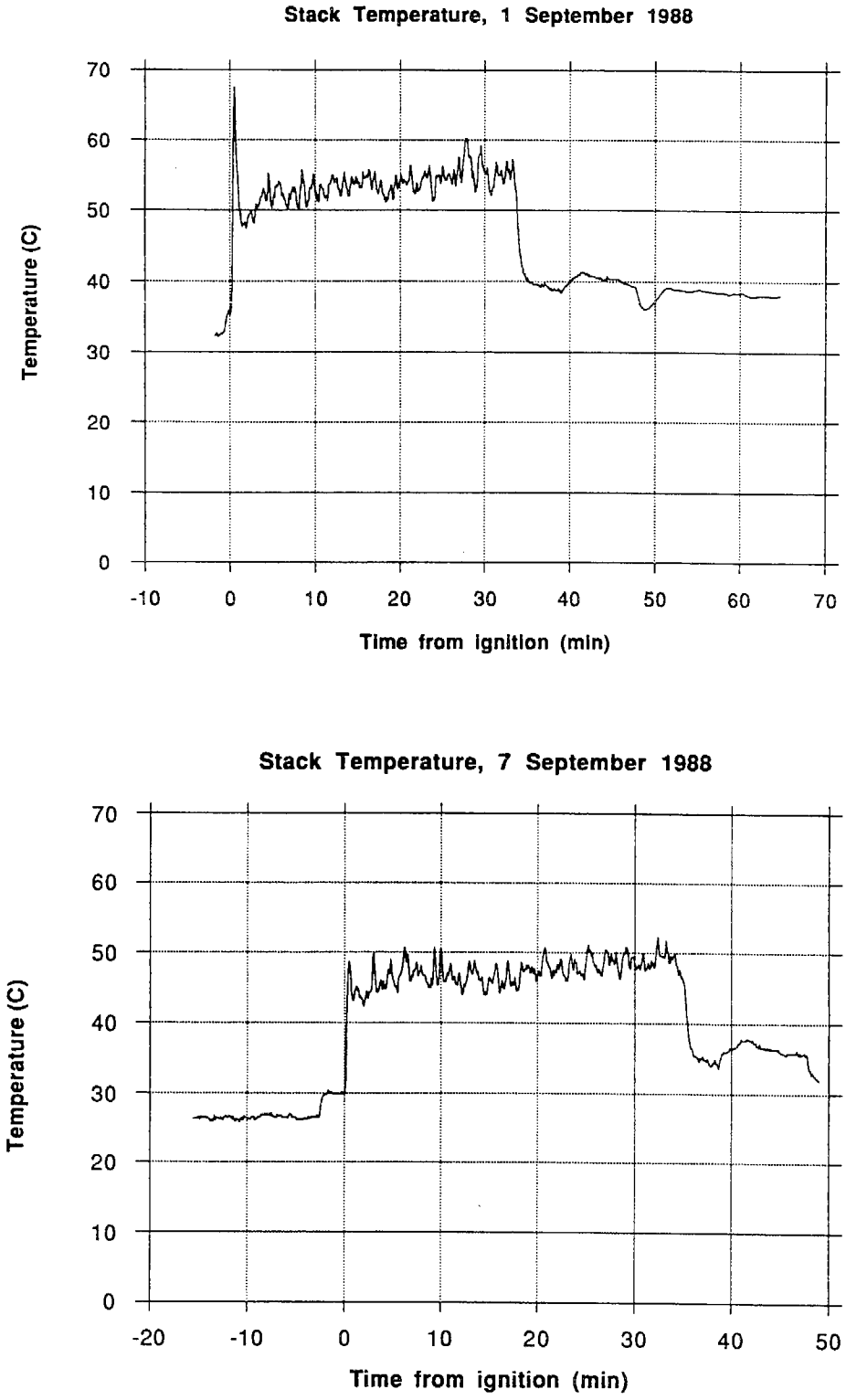

Fig. 17. Stack temperatures at the sampling port during the tests of 1 and 7 September, 1988.

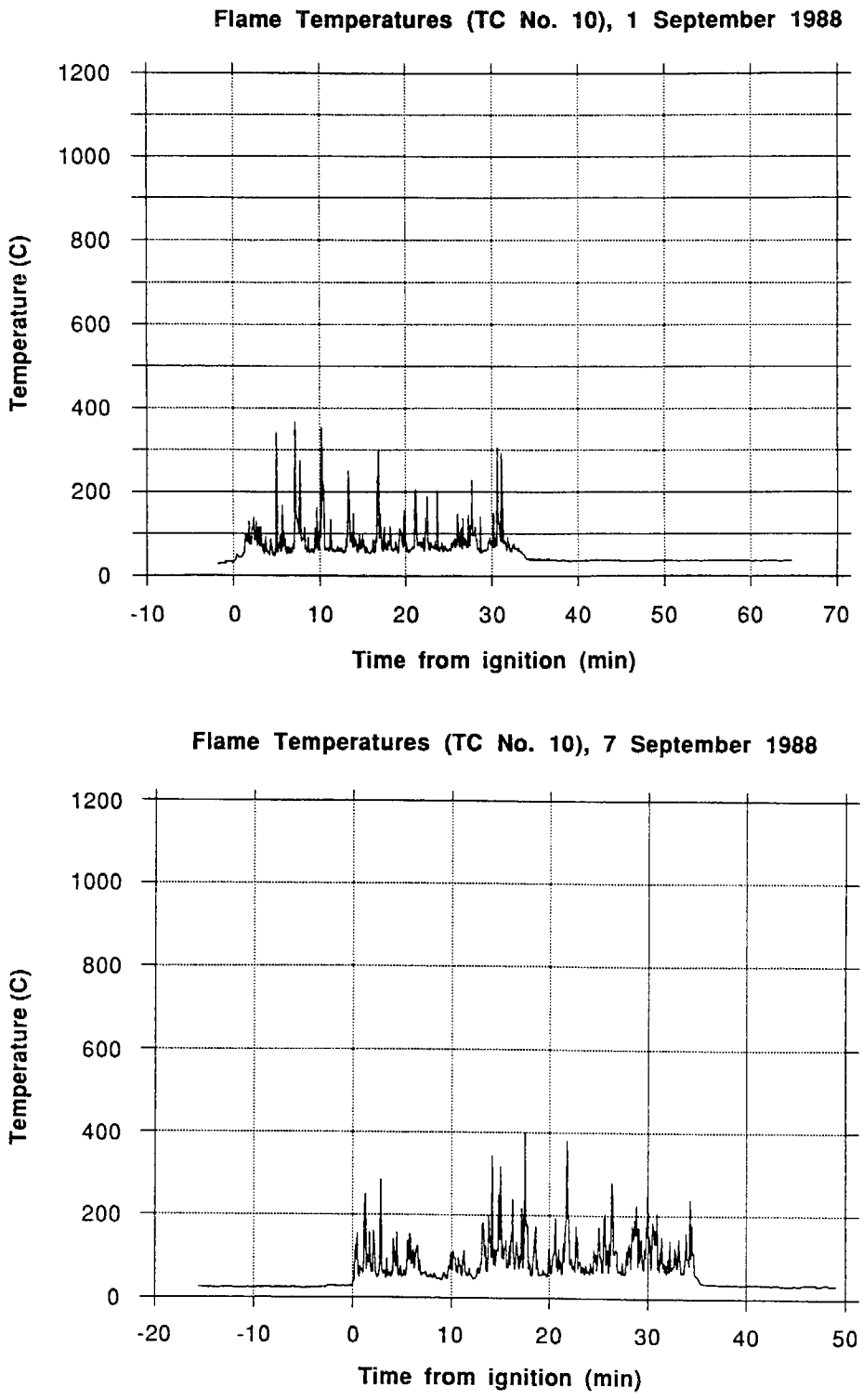

Fig. 18. Temperatures measured at 216 mm above the leading edge of the fire during the tests of 1 and 7 September, 1988.

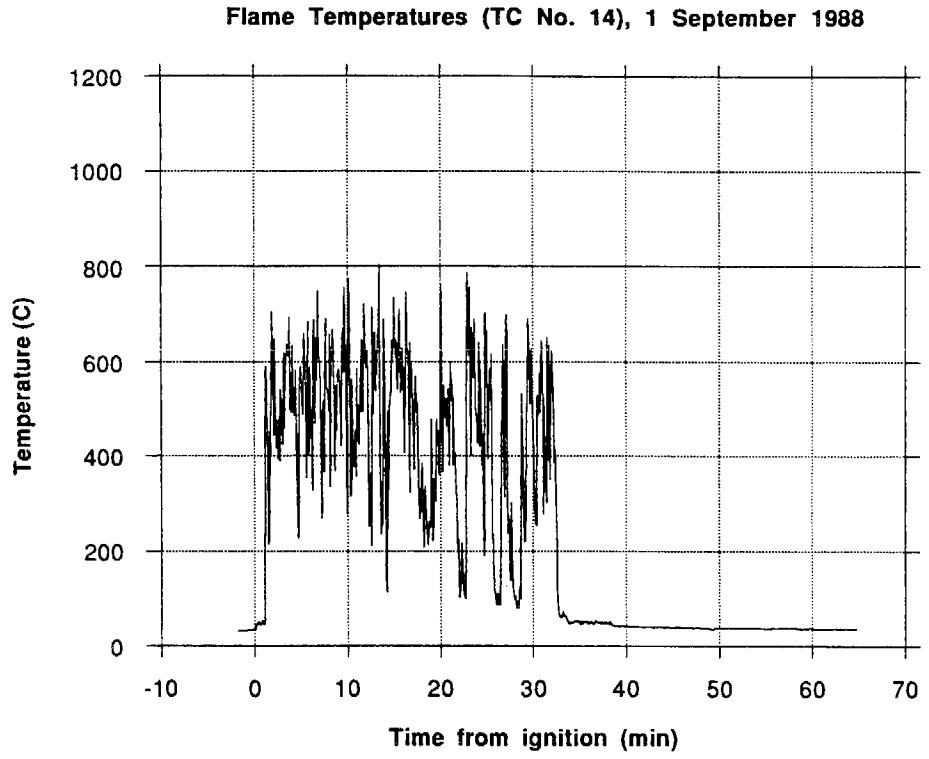

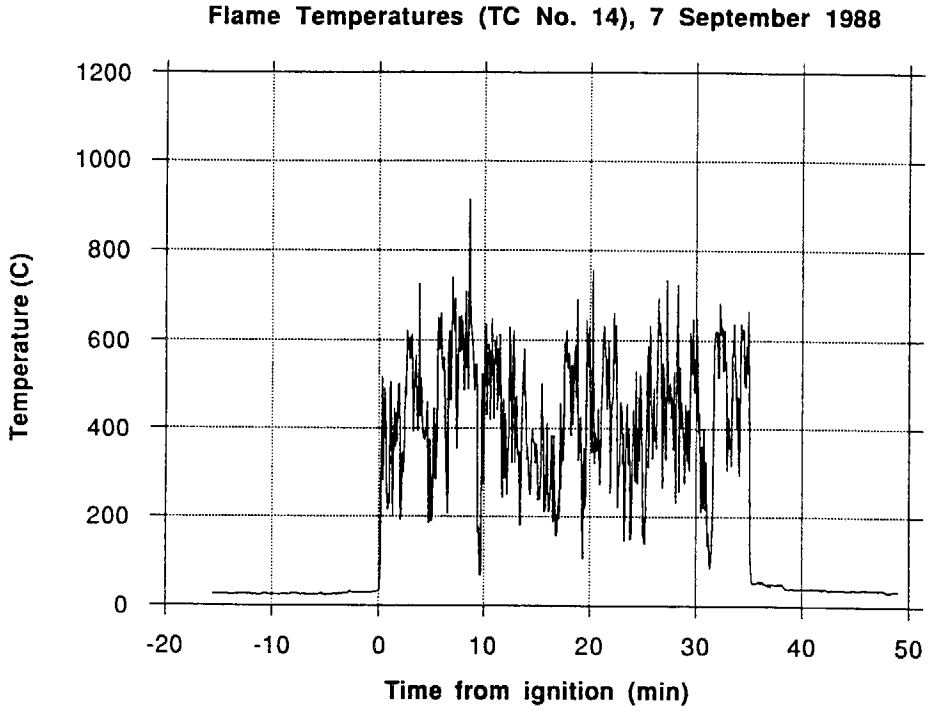

Fig. 19. Temperatures measured at 44 mm above the leading edge of the fire during the tests of 1 and 7 September, 1988.

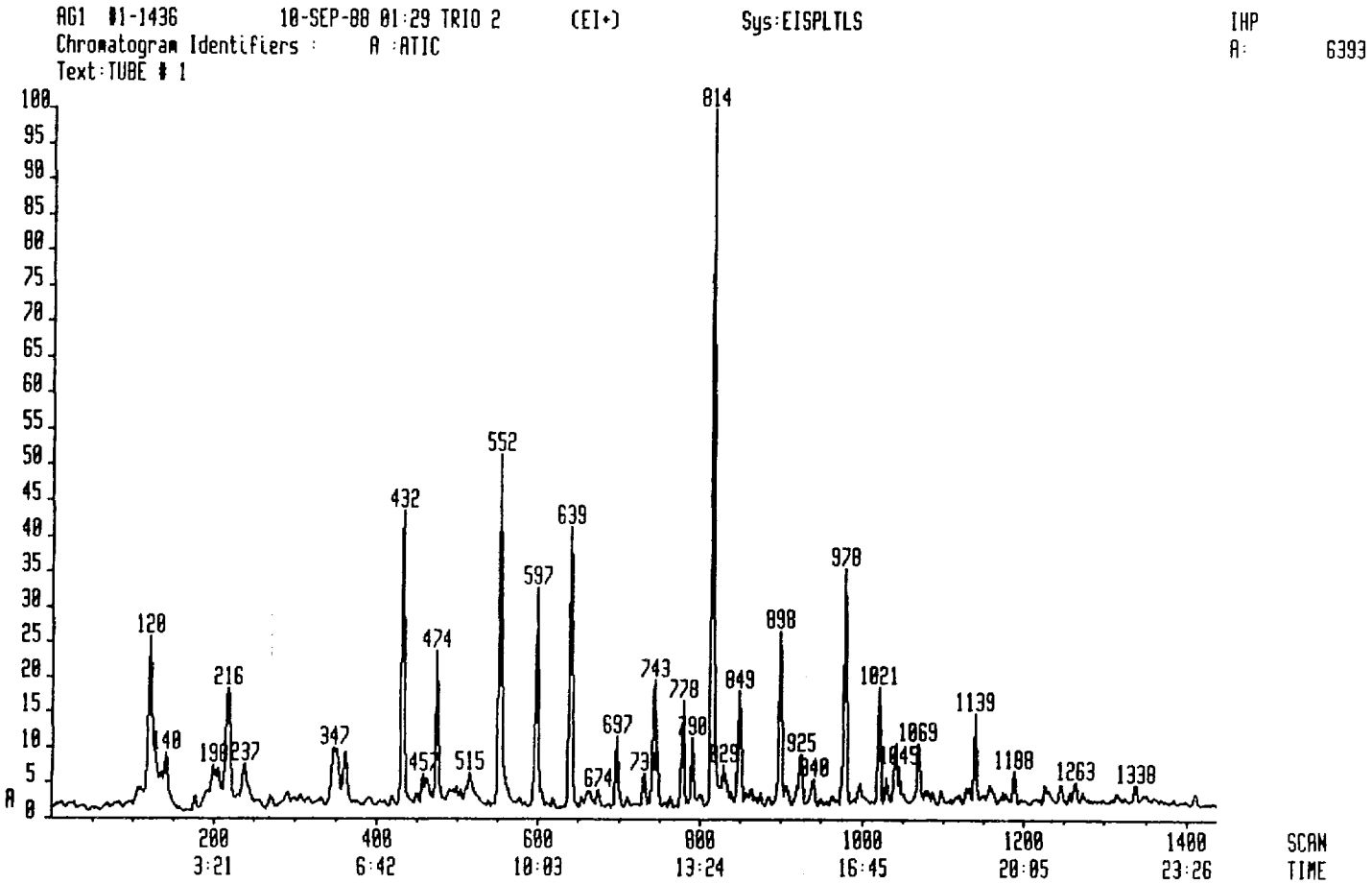

Fig. 20. Sample chromatogram (sorbent tube #1) taken during the test of 7 September and analyzed by GC-MS.

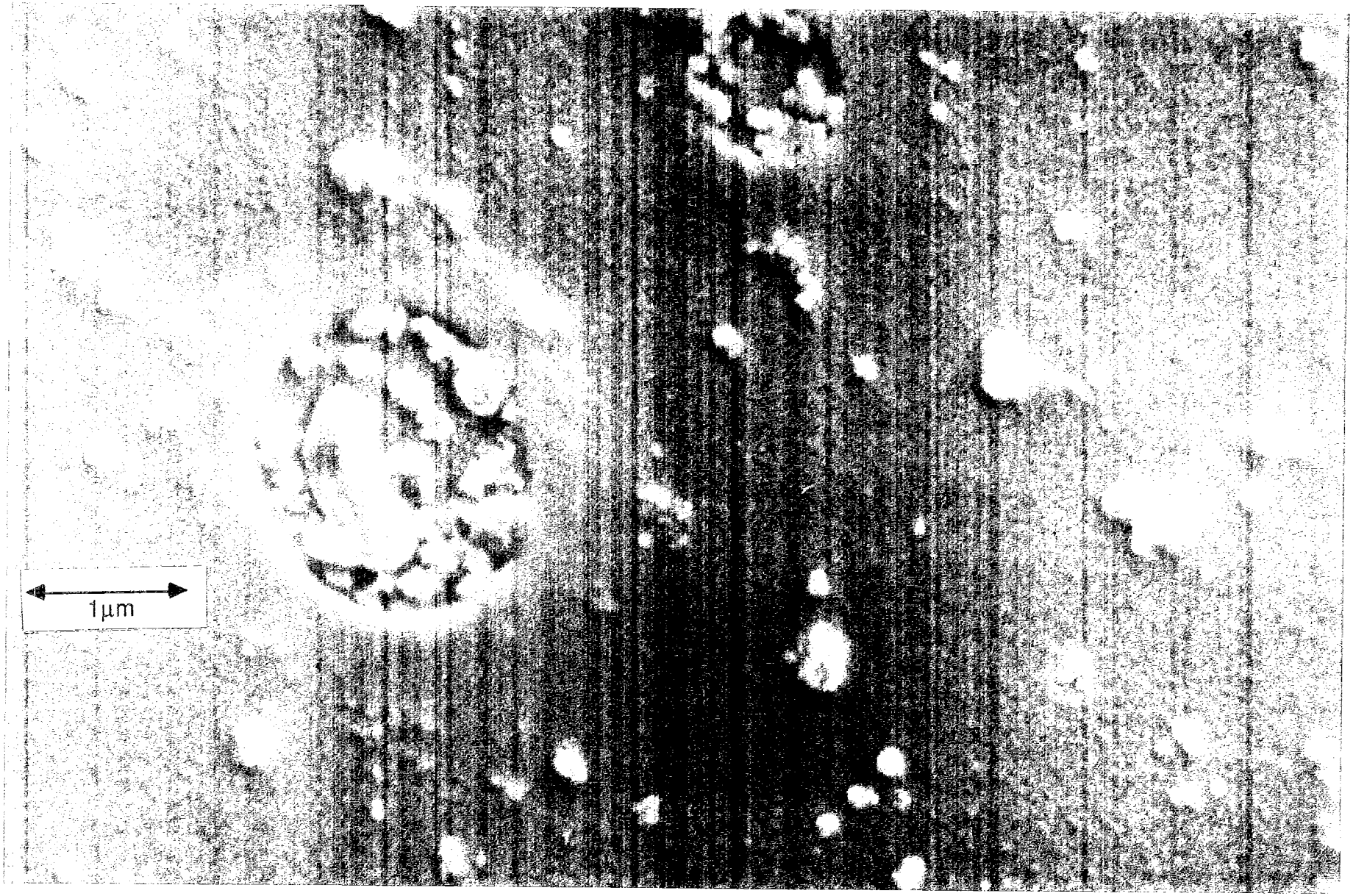

Fig. 21. Scanning electron micrograph of sample drawn from the pyrolysis zone of the fire. Sample was collected with a point to plane electrostatic precipitator on a carbon coated electron microscope grid. Residues of droplets containing solid material are visible.

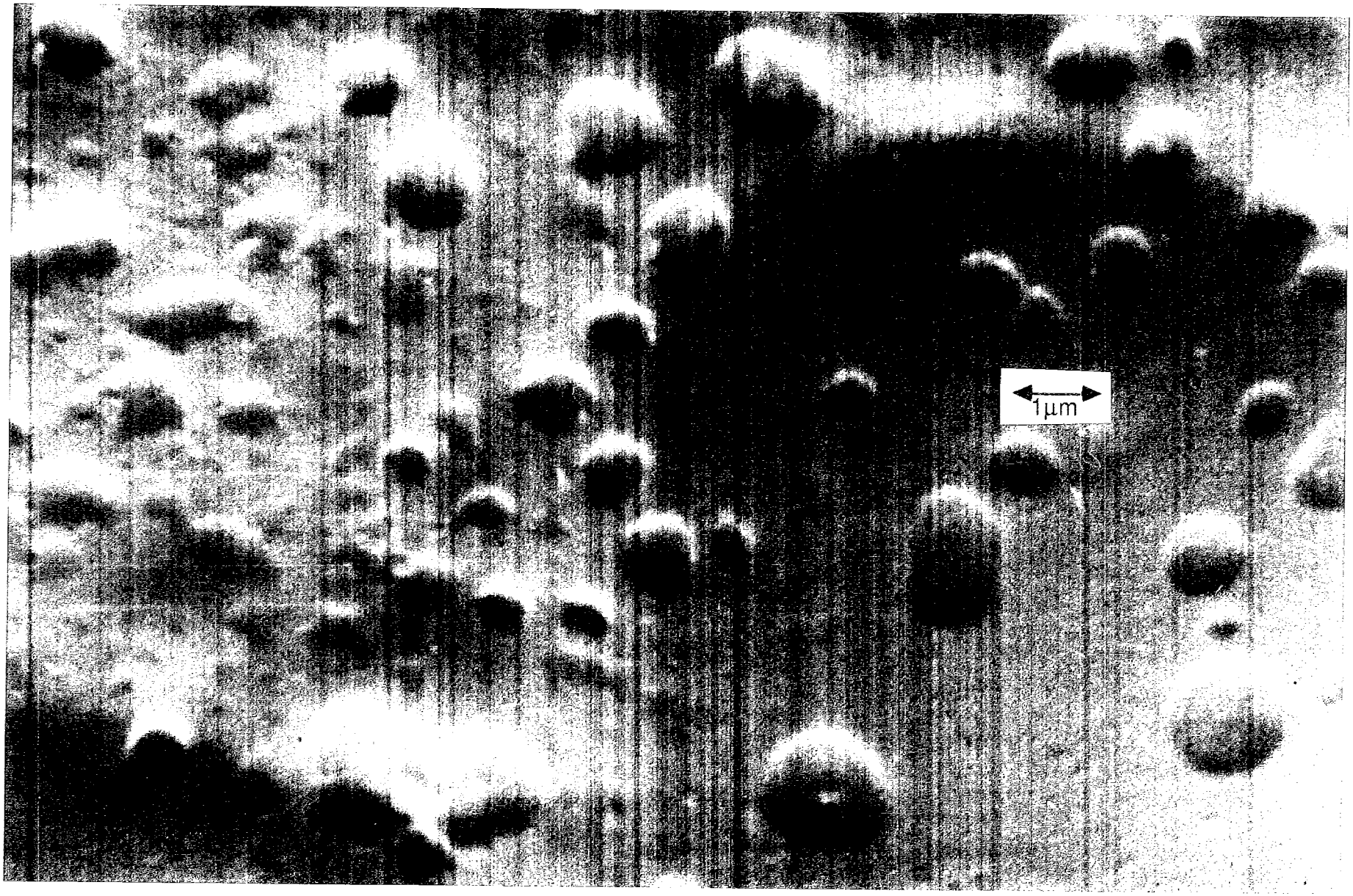

Fig. 22. Scanning electron micrograph of sample drawn from the pyrolysis zone of the fire. Sample was collected with a point to plane electrostatic precipitator on a carbon coated electron microscope grid. Residues of fine droplets are visible.

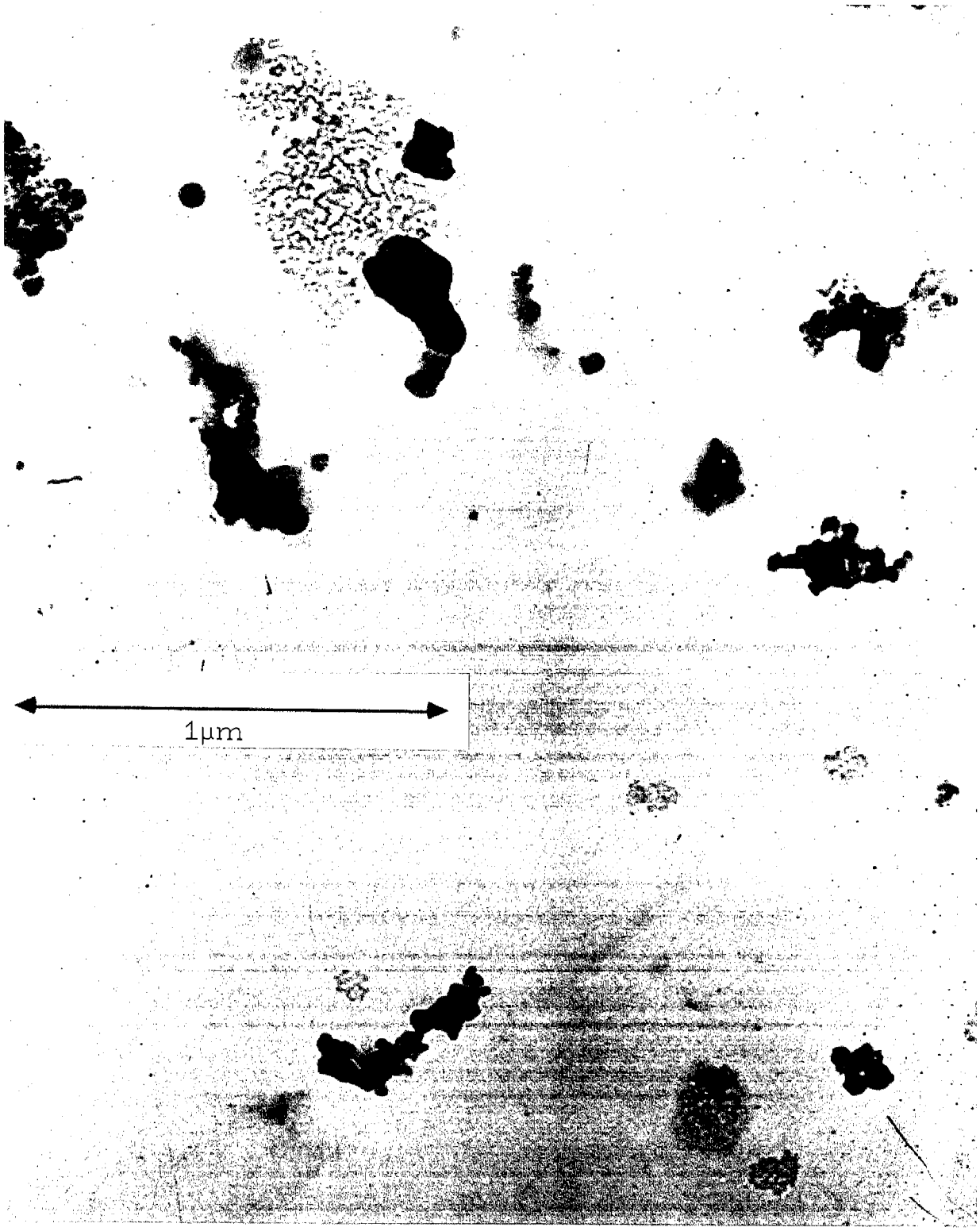

Fig. 23. Transmission electron micrograph of particulate material collected from the pyrolysis zone of the fire. Fine chain aggregate along with droplet residues are visible.

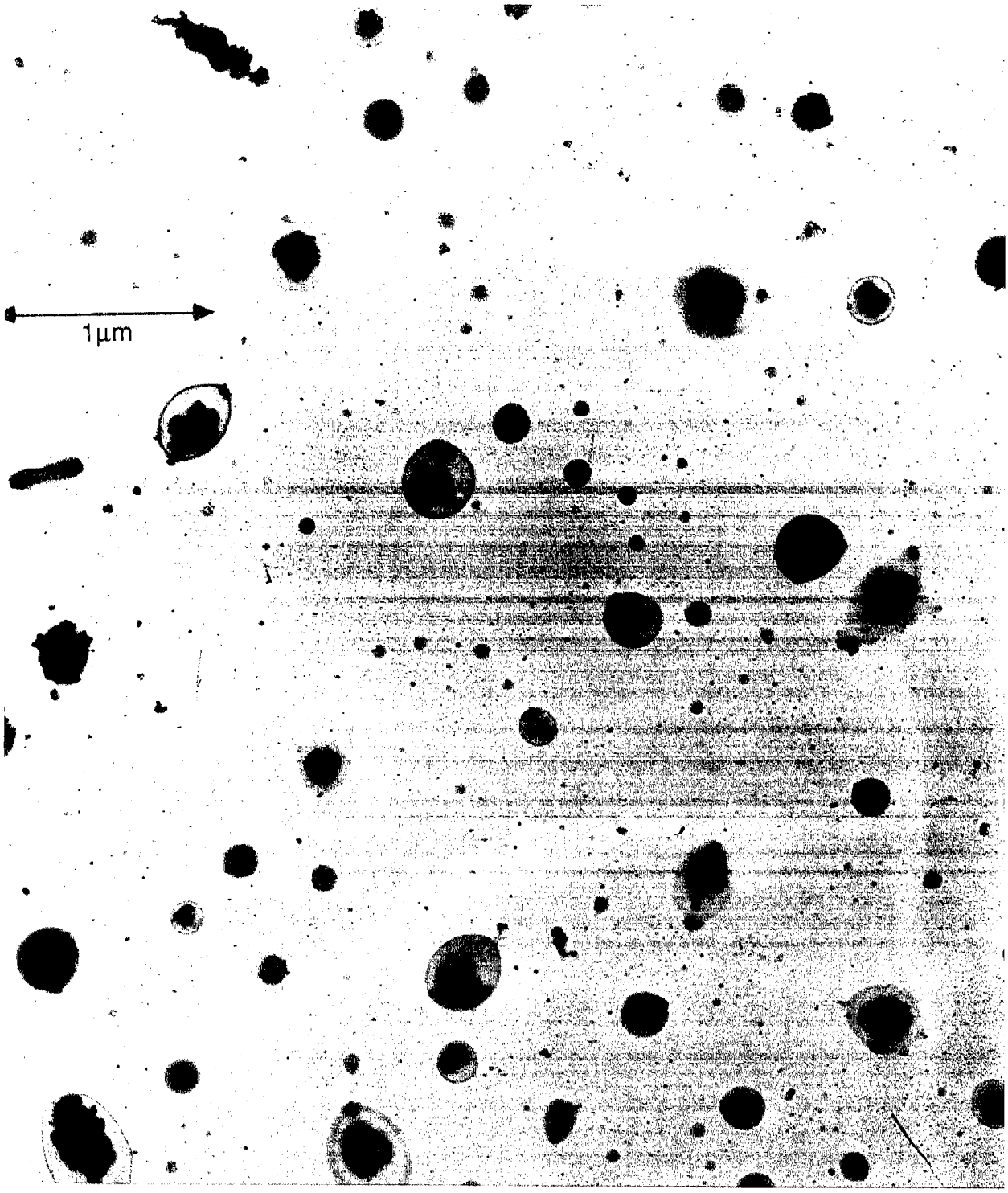

Fig. 24. Transmission electron micrograph of particulate material collected from the pyrolysis zone of the fire. Residues from fine droplets containing solid material are visible.

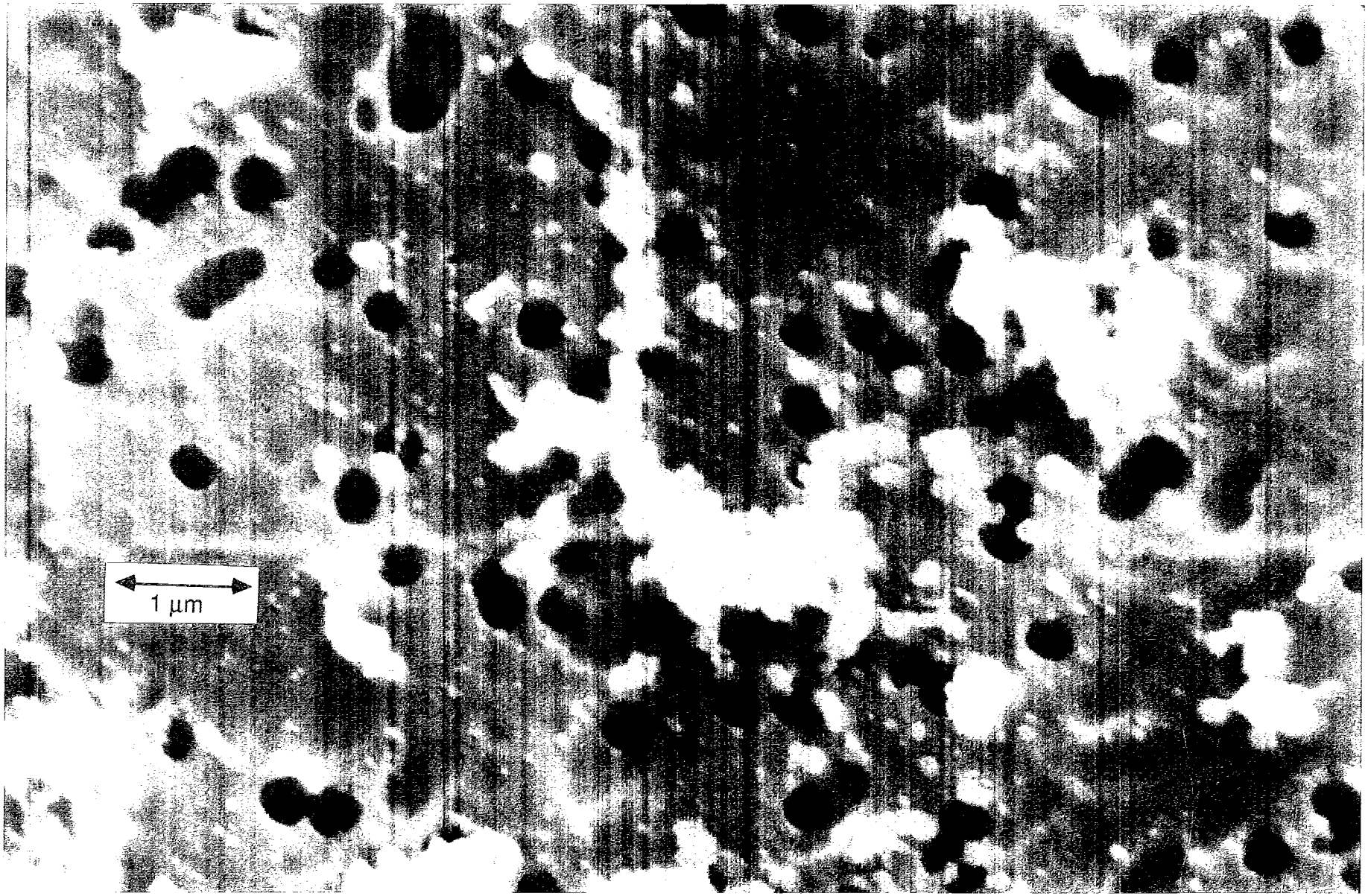

Fig. 25. Scanning electron micrograph of samples from behind the flame collected on a Nuclepore filter and showing fine chain aggregate.

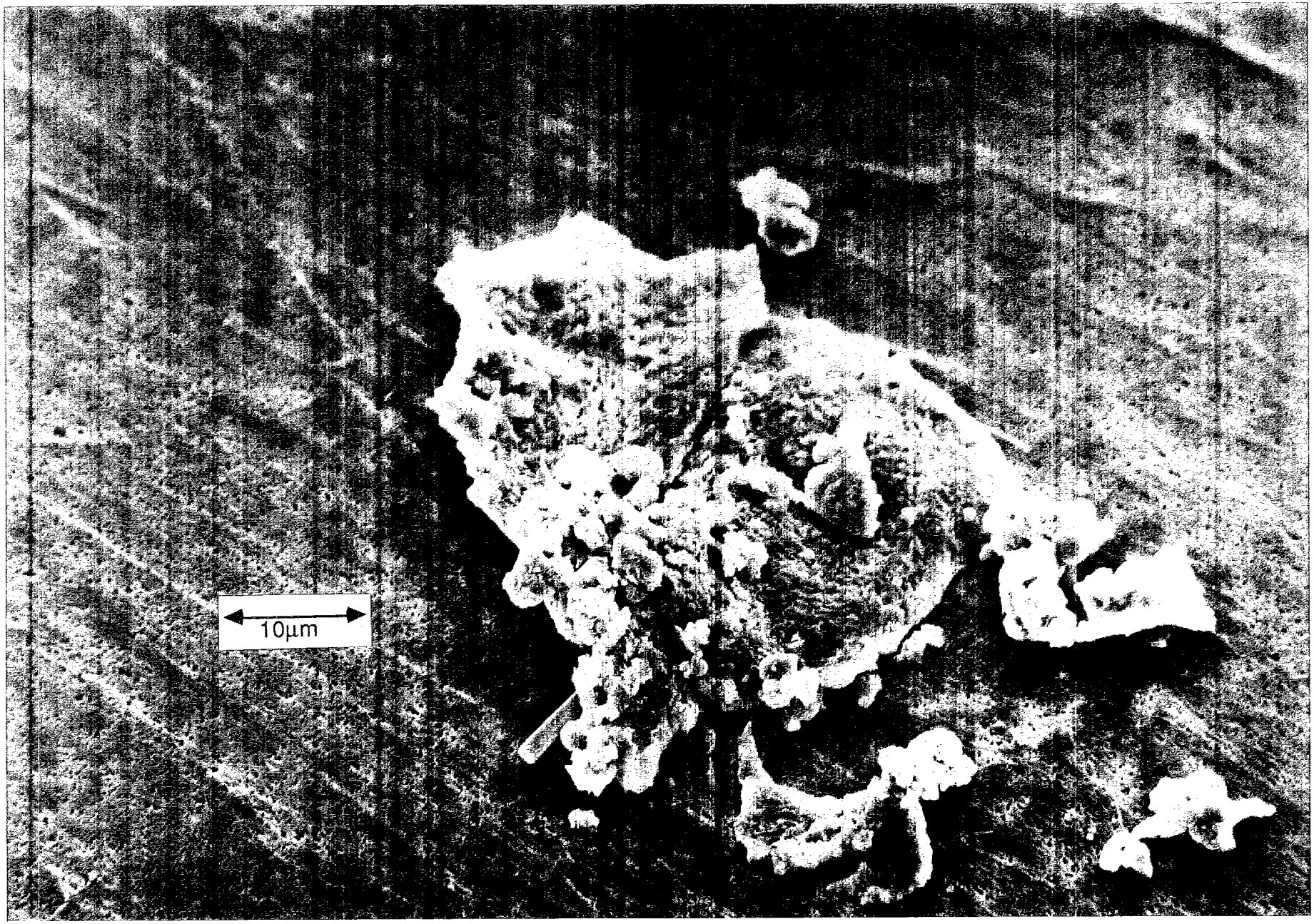

Fig. 26. Scanning electron micrograph of samples from behind the flame collected on a Nuclepore filter. Visible is a large flyash particle with other combustion particles aggregated on its surface.

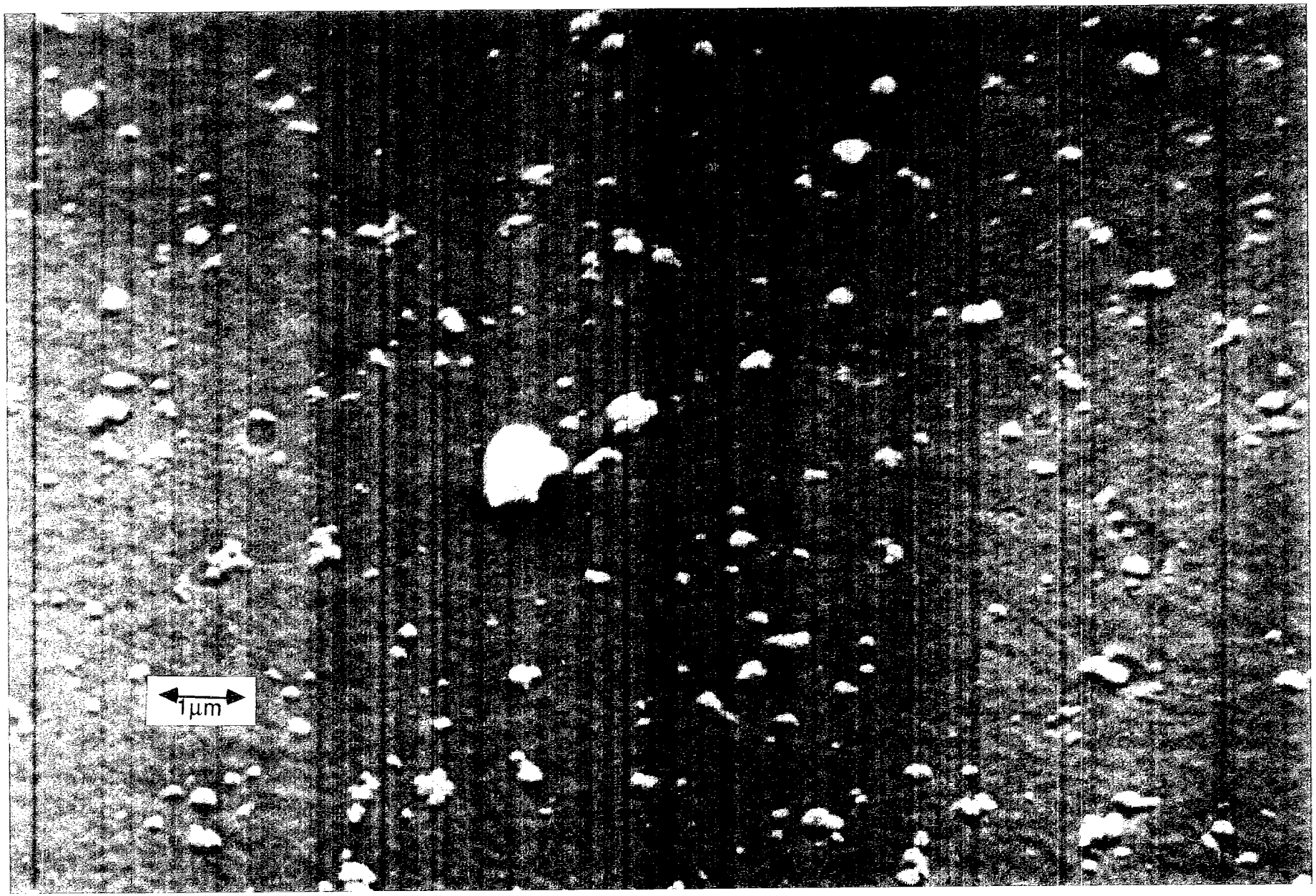

Fig. 27. Scanning electron micrograph of sample drawn from the incandescent region of the fire behind the flame in the fuel bed. Sample was collected with a point to plane electrostatic precipitator on a carbon coated electron microscope grid.

Fig. 28. Transmission electron micrograph of sample drawn from the incandescent region of the fire behind the flame in the fuel bed. Sample was collected with a point to plane electrostatic precipitator on a carbon coated electron microscope grid.